# Outline: Relativistic Coulomb excitation

Lecturer: Hans-Jürgen Wollersheim

e-mail: h.j.wollersheim@gsi.de

web-page: https://web-docs.gsi.de/~wolle/ and click on

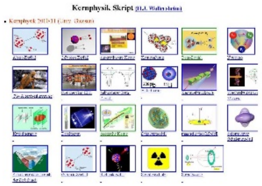

1. production, separation, identification of RIBs
2. scattering experiments at relativistic energies
3. relativistic Coulomb excitation
4. Doppler shift correction
5. experimental results with RIBs

# Physics with exotic nuclei

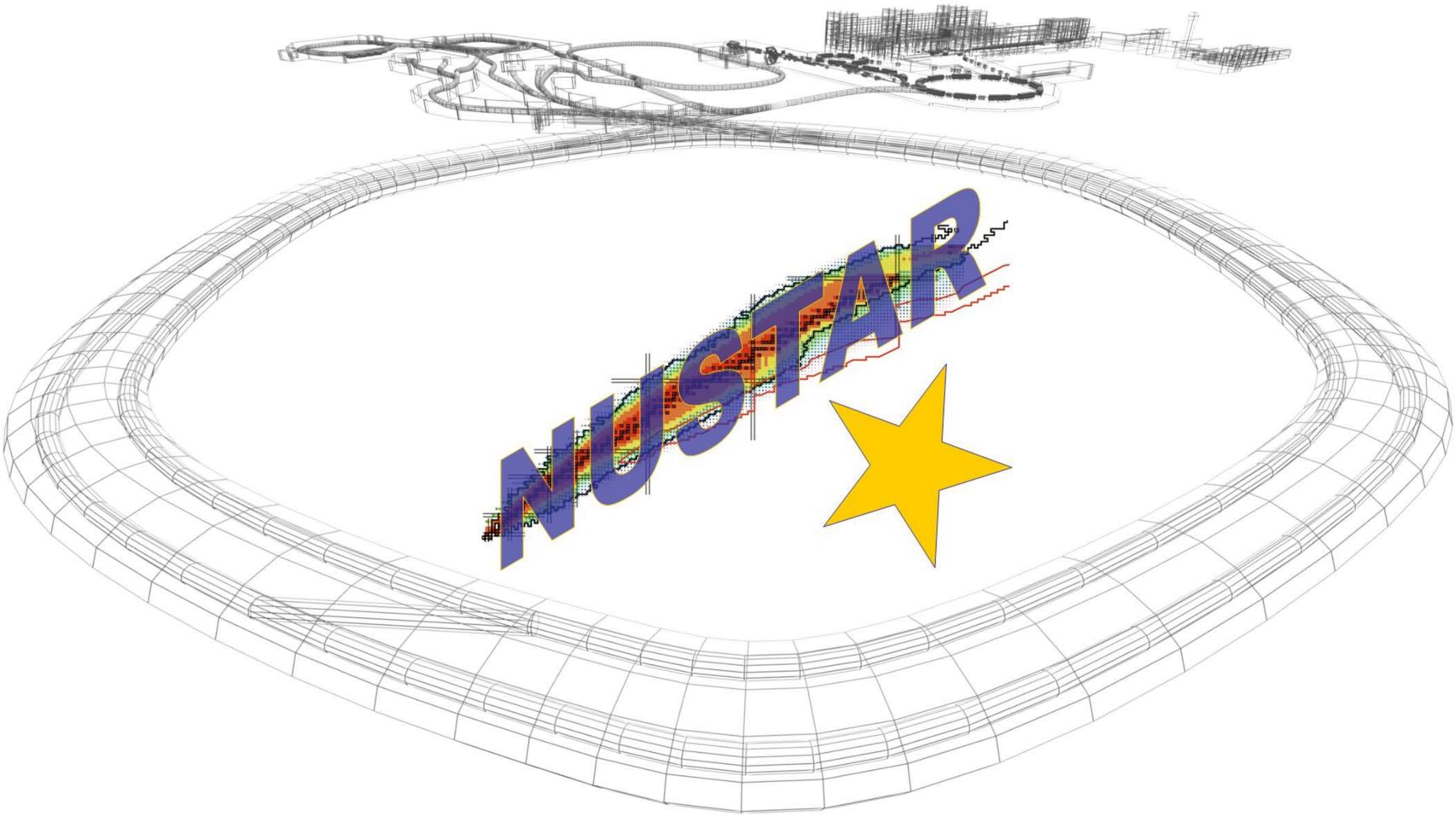


**NUclear STructure, Astrophysics and Reactions**

# High-energy Coulomb excitation

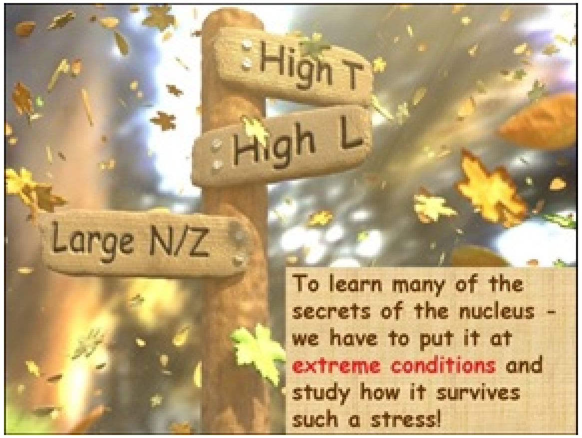


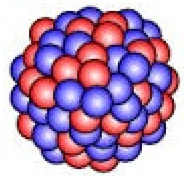

## SIS-18

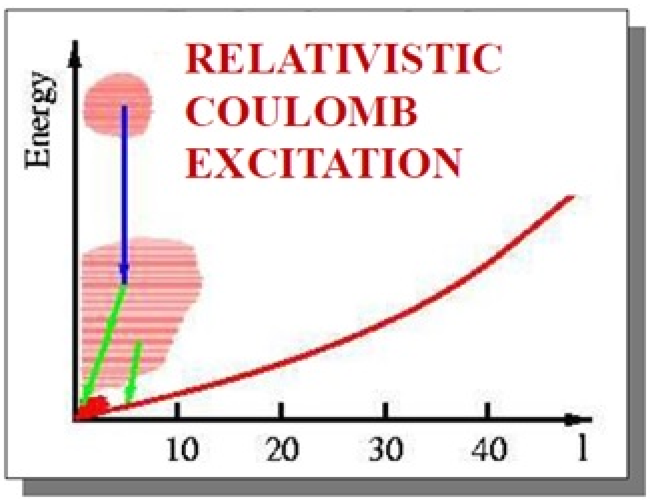


## UNILAC

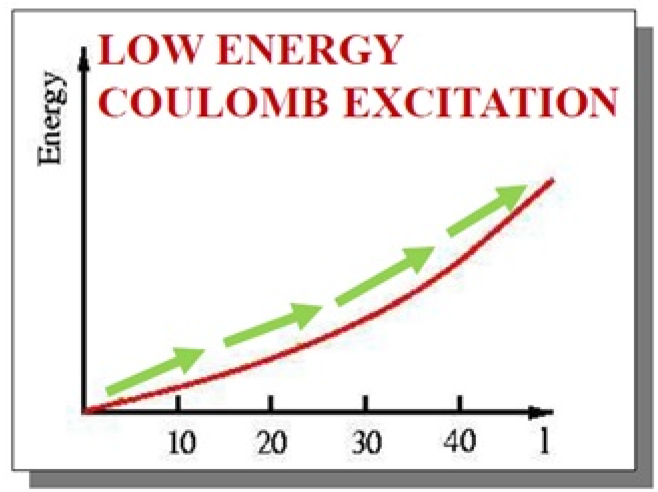

# High-energy Coulomb excitation – energy transfer and angular momentum transfer

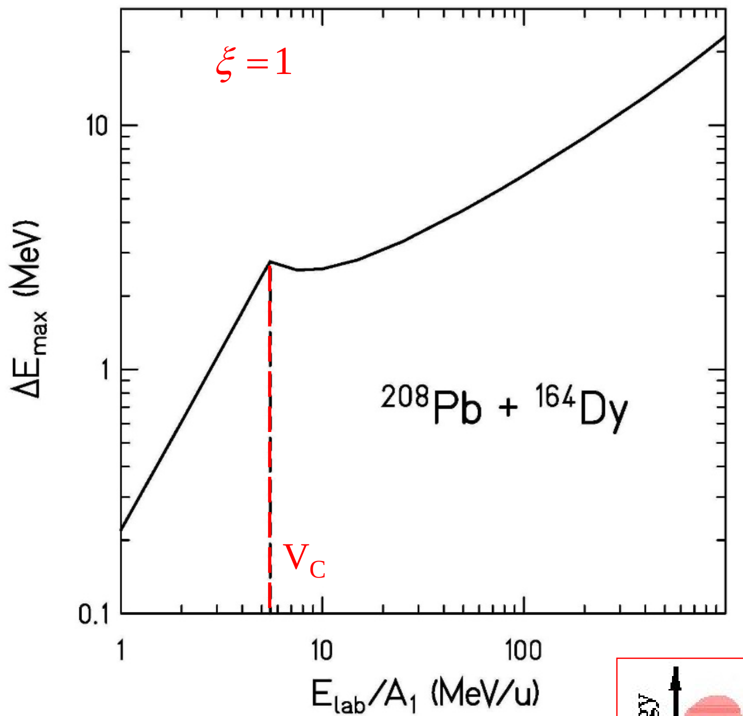


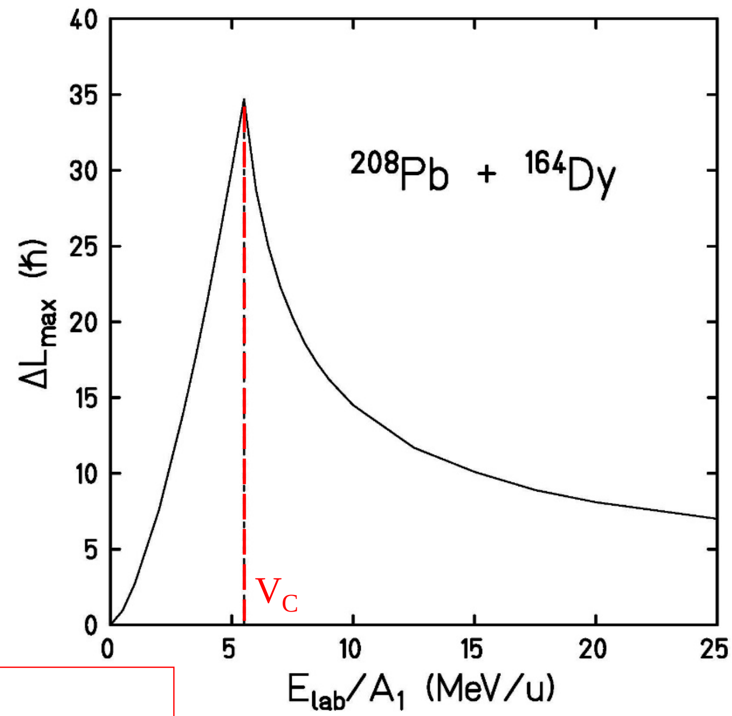


***energy transfer*** (for single-step e

$$\Delta E_{exc} = \hbar \cdot c \cdot \frac{\beta \cdot \gamma}{D - a}$$

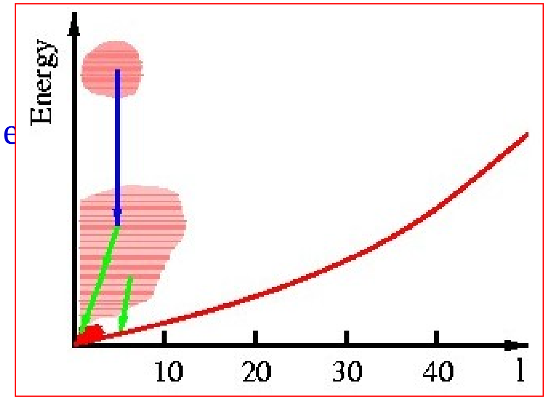


***angular momentum transfer:***

$$\Delta L_{max} \cong \frac{Z_P \cdot e^2 \cdot Q_0}{4 \cdot \hbar \cdot v \cdot a^2} \cdot (1 - cos\theta_{cm})$$

# Experimental evidence for magic numbers close to stability

S. Raman et al., Atomic Data & Nuclear Data Tables 78, 1

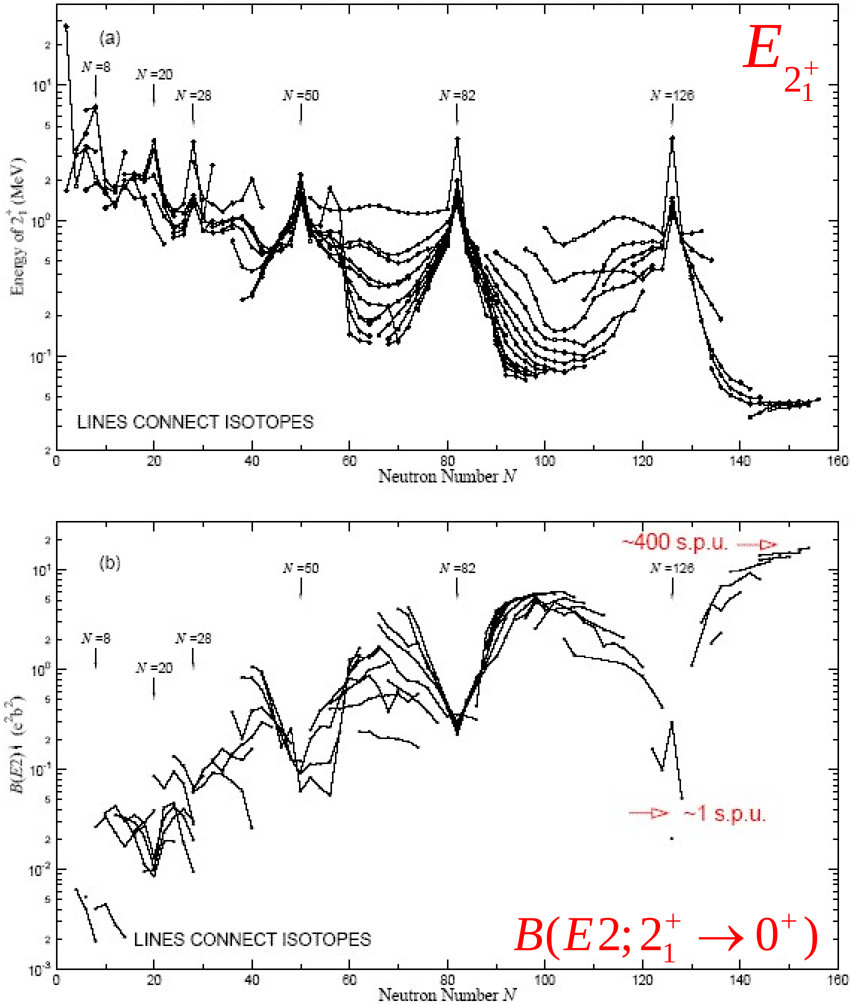


**Table 1 -- Nuclear Shell Structure** (from *Elementary Theory of Nuclear Shell Structure*, Maria Goeppert-Mayer & J. Hans D. Jensen , John Wiley & Sons, Inc., New York, 1955.)

| Angular Momentum ($h\Omega/2\pi$) | | Spin-Orbit Coupling (1/2, 3/2, 5/2, 7/2...) | Number of Nucleons Shell | Total | Magic Number |
|---|---|---|---|---|---|
| 7 | 1j | | | | |
| | | 1j 15/2 | 16 | [184] | {184} |
| | | 3d 3/2 | 4 | [168] | |
| 6 | 4s | 4s 1/2 | 2 | [164] | |
| 6 | 3d | 2g 7/2 | 8 | [162] | |
| | | 1i 11/2 | 12 | [154] | |
| 6 | 2g | 3d 5/2 | 6 | [142] | |
| | | 2g 9/2 | 10 | [136] | |
| 6 | 1i | | | | |
| | | 1i 13/2 | 14 | [126] | {126} |
| | | 3p 1/2 | 2 | [112] | |
| 5 | 3p | 3p 3/2 | 4 | [110] | |
| | | 2f 5/2 | 6 | [106] | |
| 5 | 2f | 2f 7/2 | 8 | [100] | |
| | | 1h 9/2 | 10 | [92] | |
| 5 | 1h | | | | |
| | | 1h 11/2 | 12 | [82] | {82} |
| 4 | 3s | 3s 1/2 | 2 | [70] | |
| | | 2d 3/2 | 4 | [68] | |
| 4 | 2d | 2d 5/2 | 6 | [64] | |
| | | 1g 7/2 | 8 | [58] | |
| 4 | 1g | | | | |
| | | 1g 9/2 | 10 | [50] | {50} |
| | | 2p 1/2 | 2 | [40] | {40} |
| 3 | 2p | 1f 5/2 | 6 | [38] | |
| | | 2p 3/2 | 4 | [32] | |
| 3 | 1f | | | | |
| | | 1f 7/2 | 8 | [28] | {28} |
| | | 1d 3/2 | 4 | [20] | {20} |
| 2 | 2s | 2s 1/2 | 2 | [16] | |
| 2 | 1d | 1d 5/2 | 6 | [14] | |
| | | 1p 1/2 | 2 | [8] | {8} |
| 1 | 1p | 1p 3/2 | 4 | [6] | |
| 0 | 1s | 1s 1/2 | 2 | [2] | {2} |

# Experimental evidence for magic numbers close to stability

S. Raman et al., Atomic Data & Nuclear Data Tables 78, 1

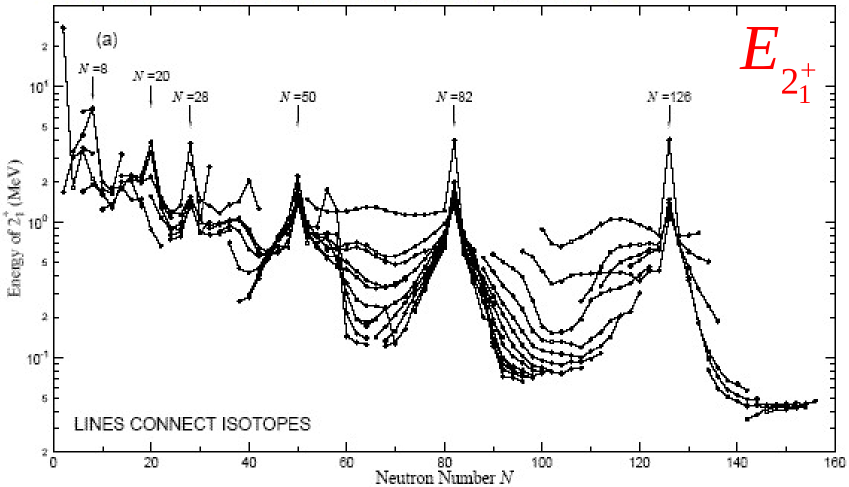


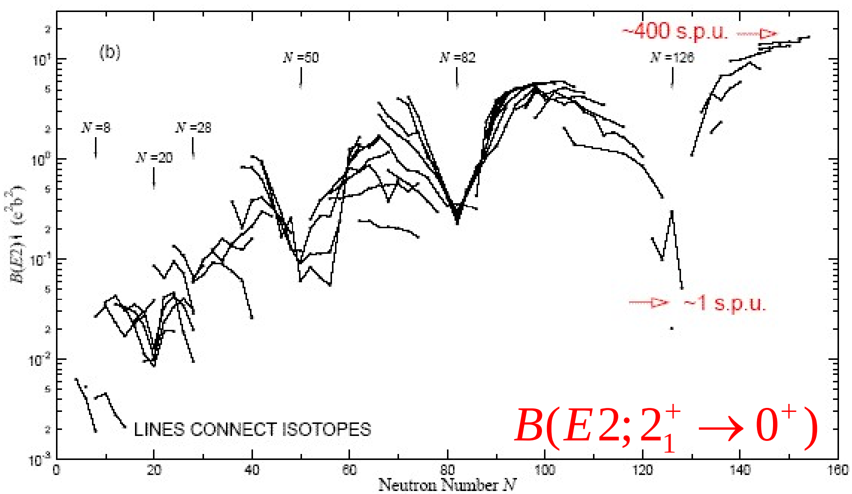


Nuclei with magic numbers of neutrons/protons

high energy of $2_1^+$ state

low $B(E2; 2_1^+ \rightarrow 0^+)$ values

**transition probability measured in single particle units (spu)**

If we move away from stability?

# Production, Separation, Identification

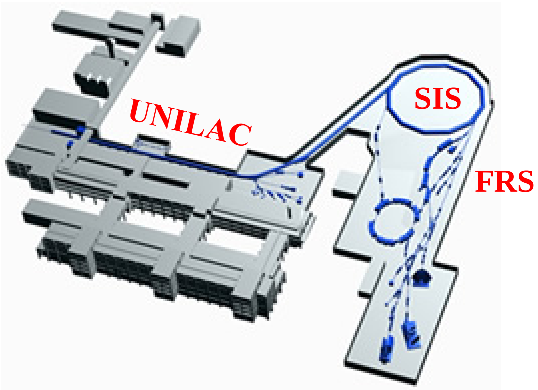


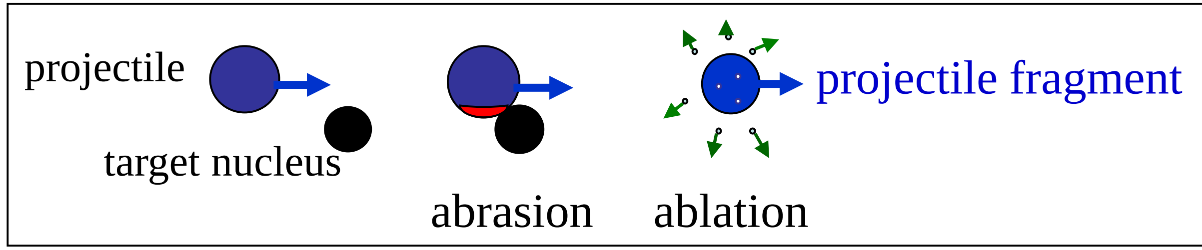


**FR**agment
**S**eparator

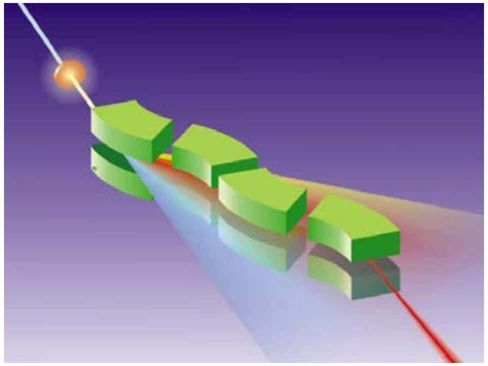

**Standard FRS detectors**

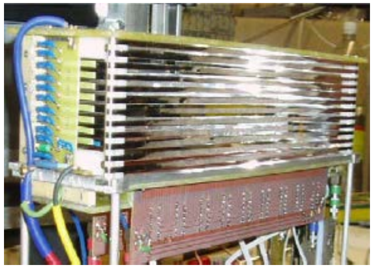

TPC-**x,y position**
@ S2,S4

Plastic scintillator
(**TOF**)
@ S4

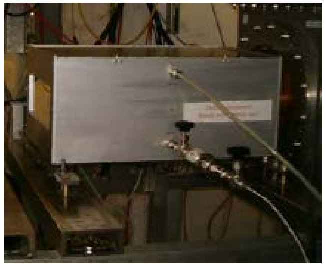

MUSIC
(**ΔE**)
@ S4

# Scattering experiments at relativistic energies

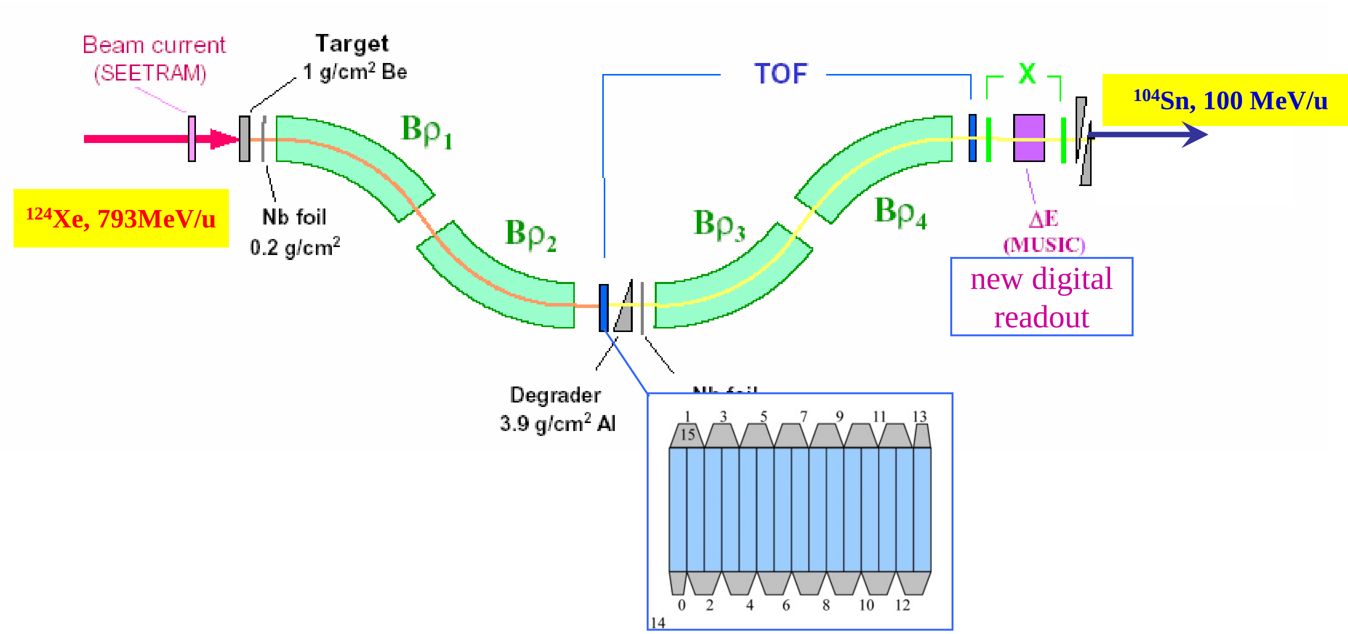


finger segmented detector

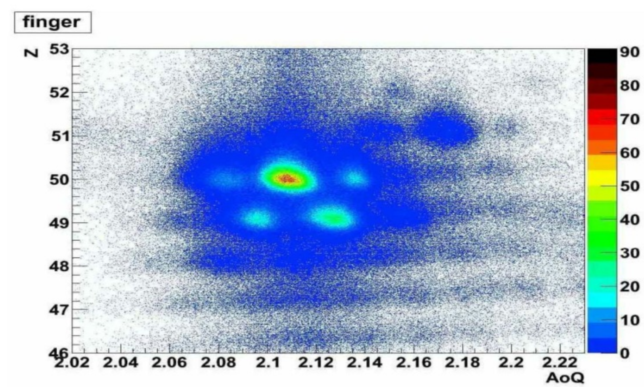


$^{104}$Sn fragments

using $^{124}$Xe at 793 MeV/u

**high rate at S2 ~$10^6$ s$^{-1}$**

- ~2400 % more tracking efficiency
- good A/Q resolving power

*Frederic Ameil*

# Scattering experiments at relativistic energies

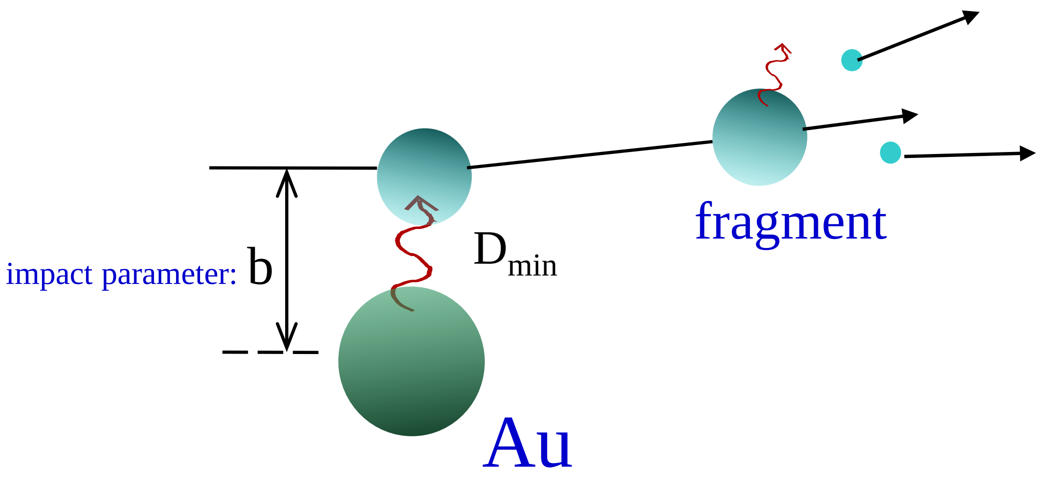


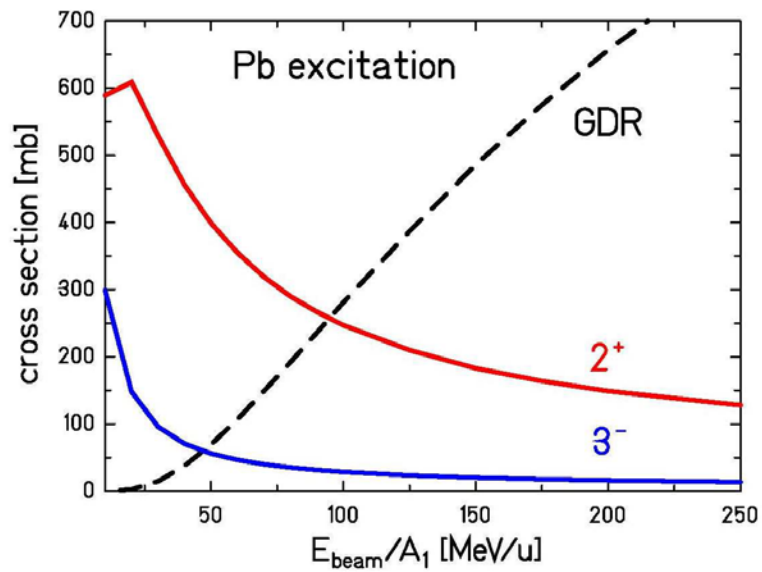


Rutherford scattering only if distance of closest approach $D_{min}$ is large compared to nuclear radii + surfaces:

$$D_{\min} > C_P + C_T + 5 \ \ fm$$

$C_P$, $C_T$ half-density radii

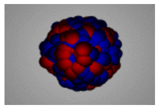

$E^* \cong 13.3\, MeV$

$B(E1; 0 \rightarrow 1^-) \cong 0.55\, e^2 b$

$E^* = 4.086\, MeV$

$B(E2; 0 \rightarrow 2^+) = 9\, Wu$

$E^* = 2.615\, MeV$

$B(E3; 0 \rightarrow 3^-) = 34\, Wu$

$$\sigma_{\pi\lambda} \approx \left(\frac{Z_P e^2}{\hbar c}\right)^2 \cdot \frac{\pi}{e^2 b^{2\lambda-2}} \cdot B(\pi\lambda; 0 \rightarrow \lambda) \cdot \begin{cases} (\lambda-1)^{-1} & for \ \ \lambda \geq 2 \\ 2\ln(b_a / b) & for \ \ \lambda = 1 \end{cases}$$

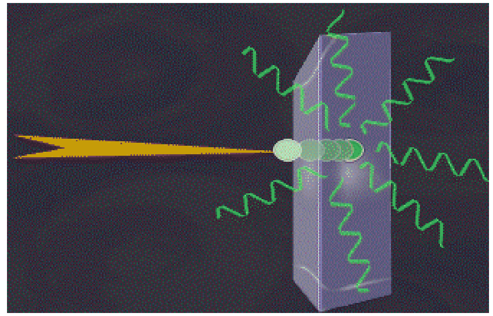

slowing down of a
moving point-charge

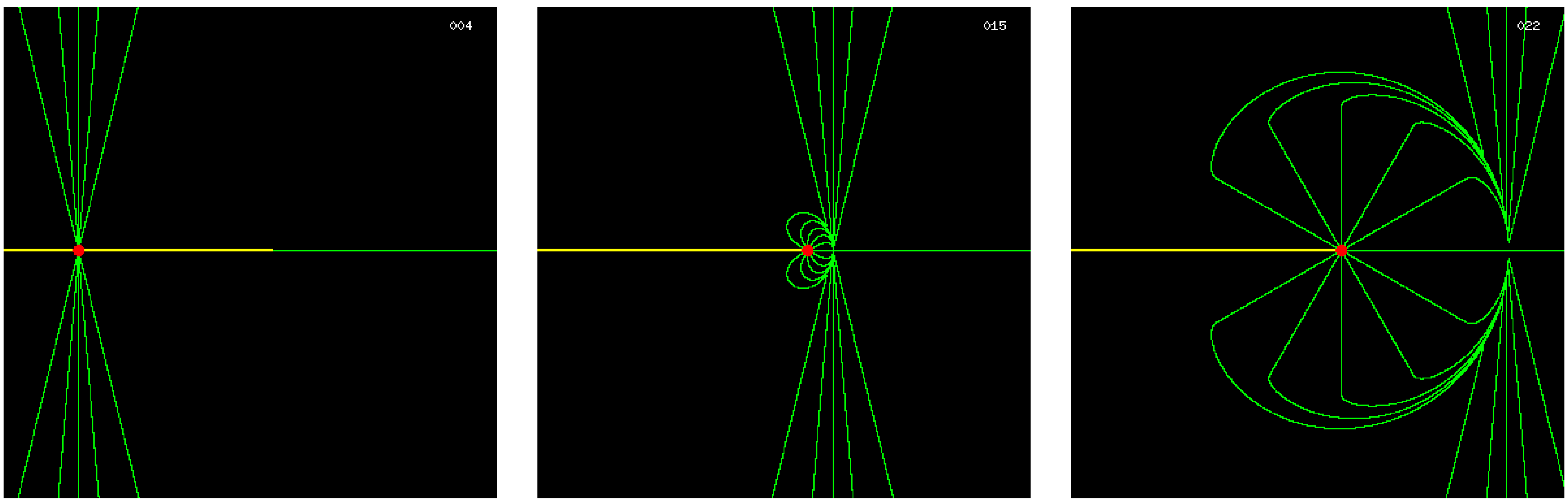


electric field lines (v/c=0.99)

# Atomic background radiation

➢Radiative electron capture (REC)
capture of target electrons into bound states of the projectile:

$$\sigma \sim Z_p^2 \cdot Z_t$$

➢Primary Bremsstrahlung (PB)
capture of target electrons into continuum states of the projectile:

$$\sigma \sim Z_p^2 \cdot Z_t$$

➢Secondary Bremsstrahlung (SB)
Stopping of high energy electrons in the target: $\sigma \sim Z_p^2 \cdot Z_t^2$

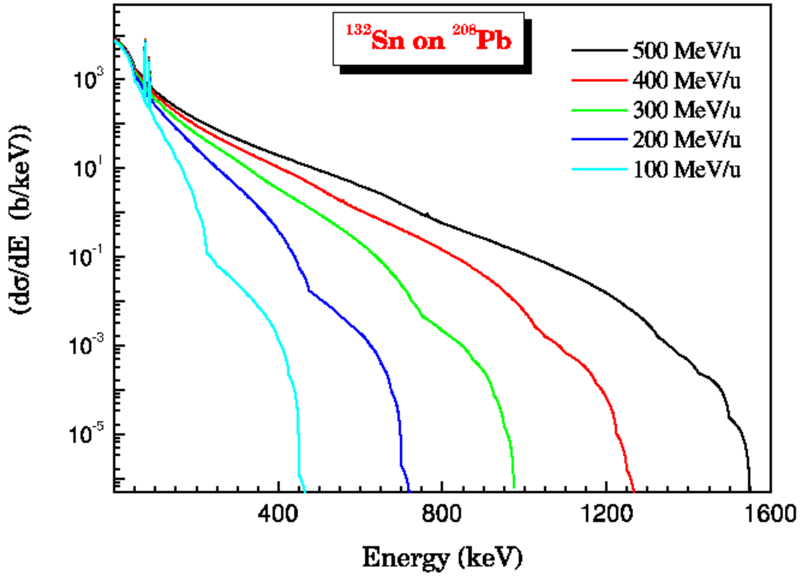


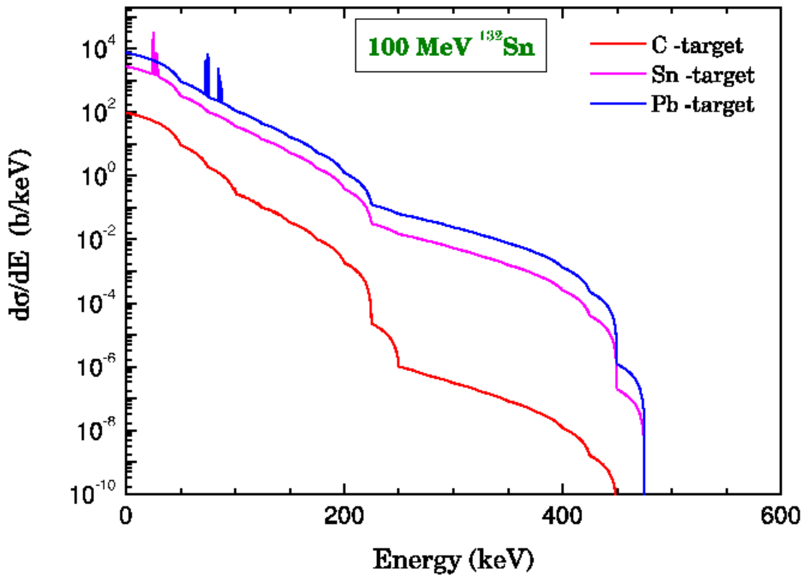


Bremsstrahlung: slowing down of a moving point-charge

# Suppression of atomic background radiation Pb & Sn absorbers

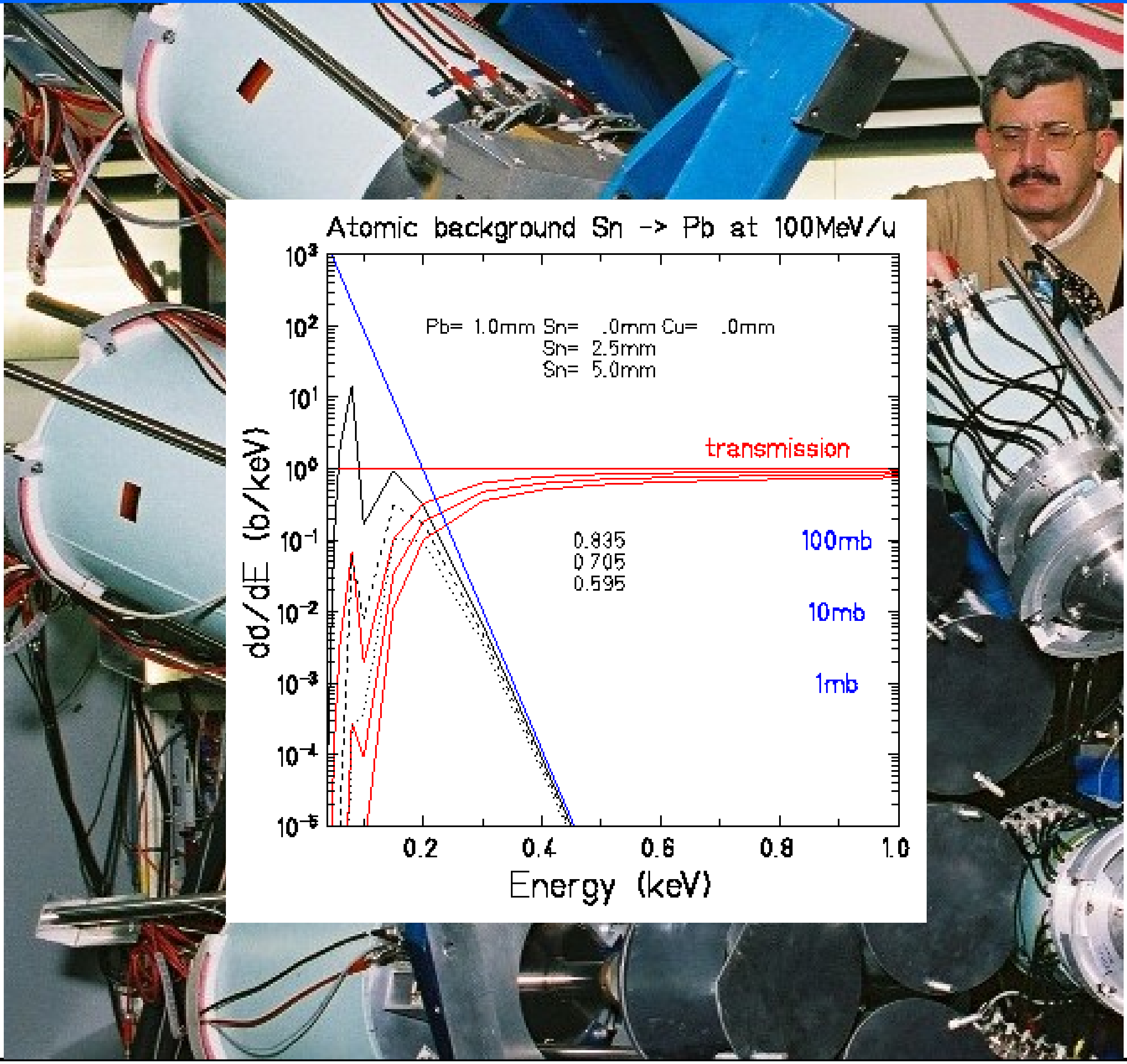

# Scattering experiment at relativistic energies

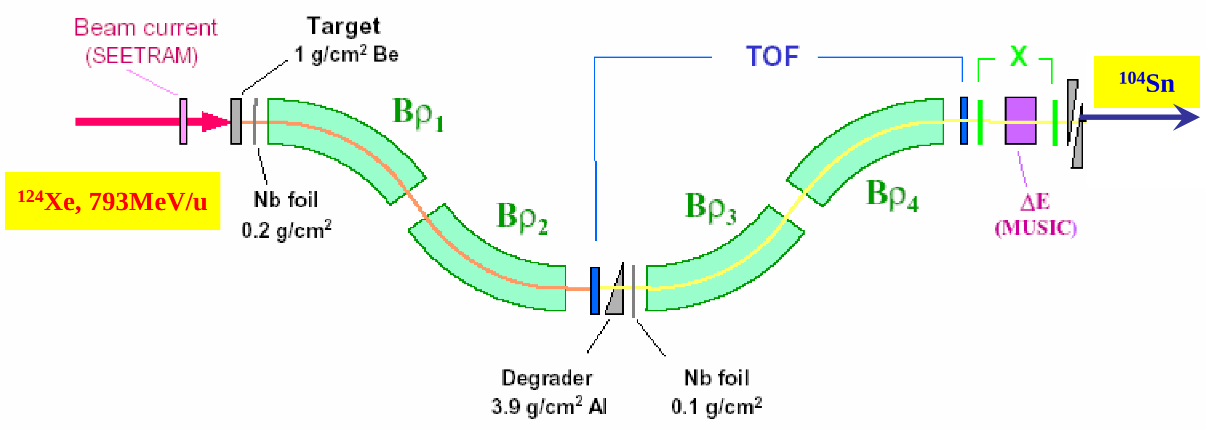


## $^{197}$Au-target

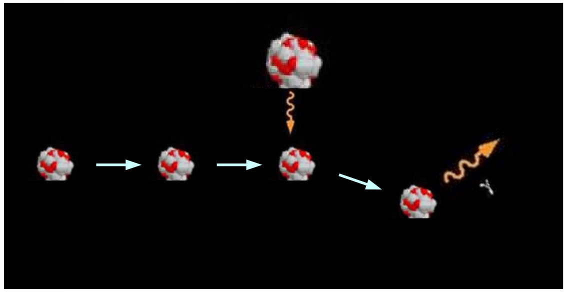

**relativistic Coulomb excitation**

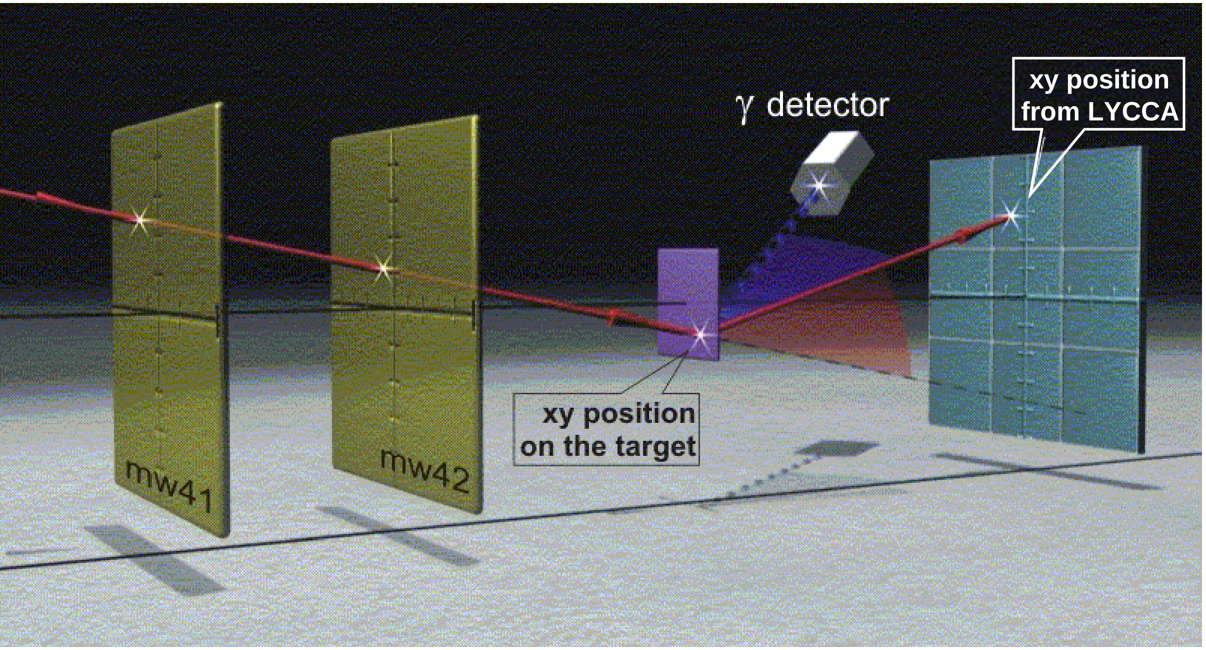

# Scattering experiment at relativistic energies

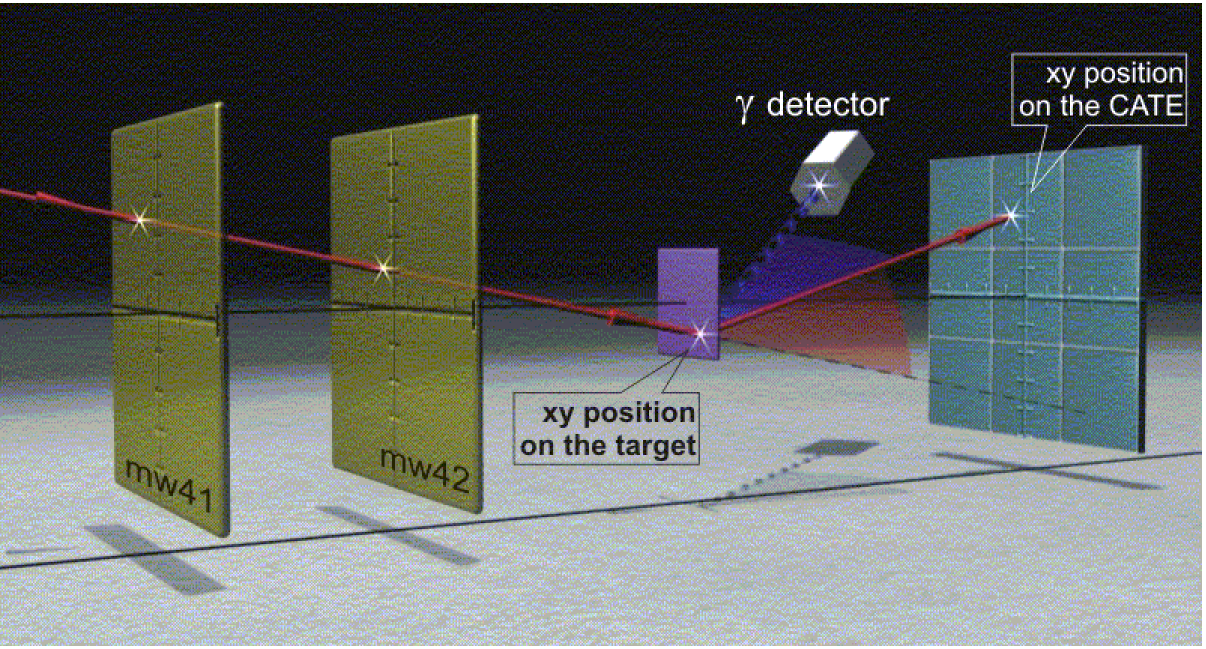


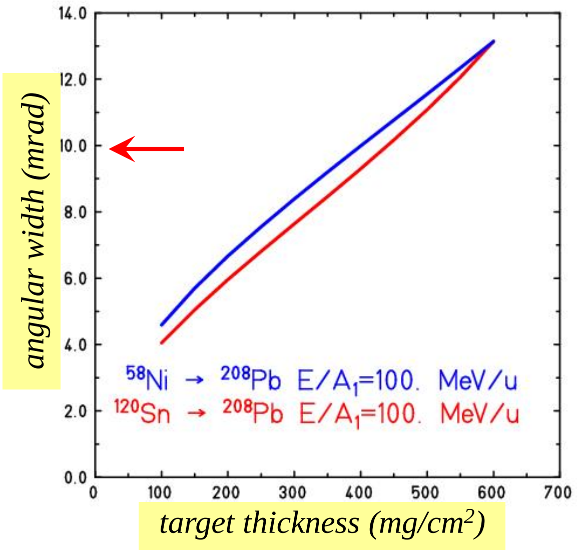


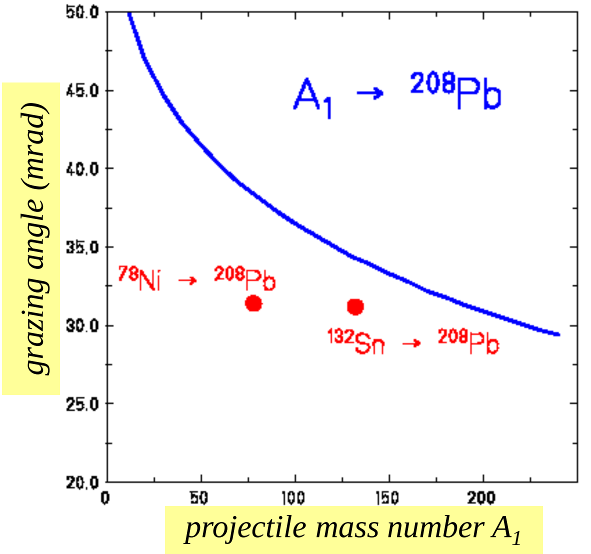


*Coulomb excitation:* $\vartheta_1^{lab} < \vartheta_{grazing}$

$$\vartheta_1^{lab} = \frac{2 \cdot Z_1 \cdot Z_2 \cdot e^2}{m_0 \cdot c^2 \cdot \gamma \cdot \beta^2 \cdot b} = \frac{2.88 \cdot Z_1 \cdot Z_2 \cdot [931.5 + (T/A_1)]}{A_1 \cdot [(T/A_1)^2 + 1863 \cdot (T/A_1)]} \cdot \frac{1}{b} \; [rad]$$

$$b \cong R_{int} = C_1 + C_2 + 4.49 - \frac{C_1 + C_2}{6.35} \; [fm]$$

# Scattering experiment at relativistic energies

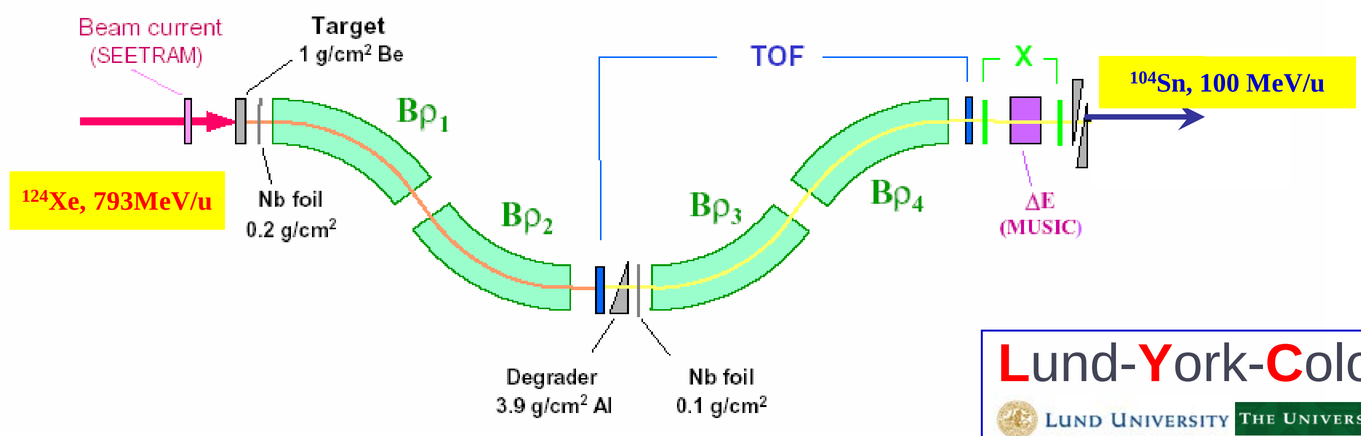


**L**und-**Y**ork-**C**ologne **CA**lorimeter

Lund University The University of York University of Cologne

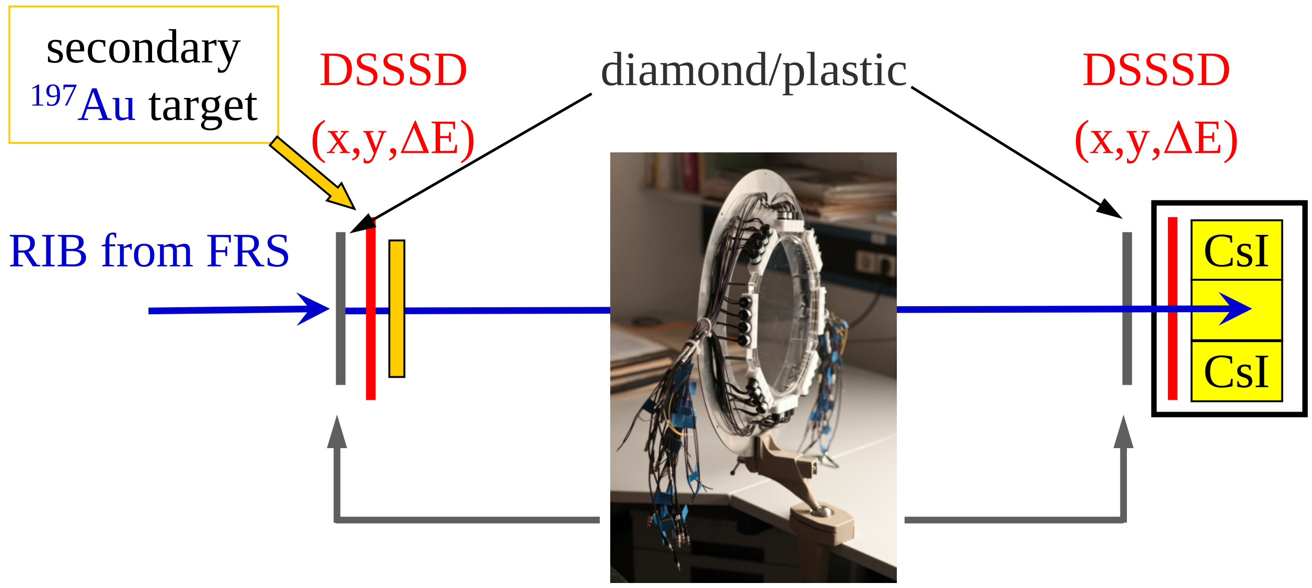


exp. observables:
**Z**, A, **θ**

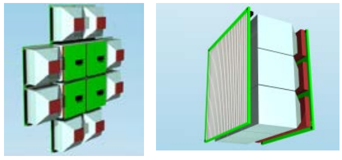



GSI

# Scattering experiment at relativistic energies

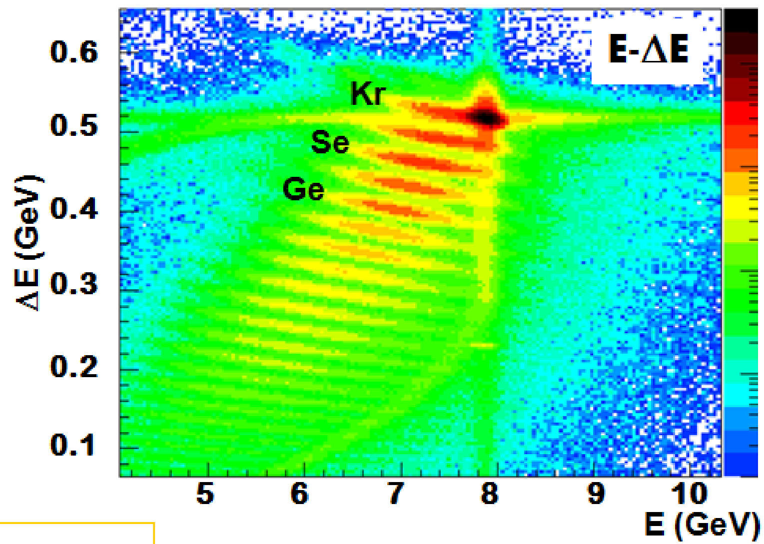


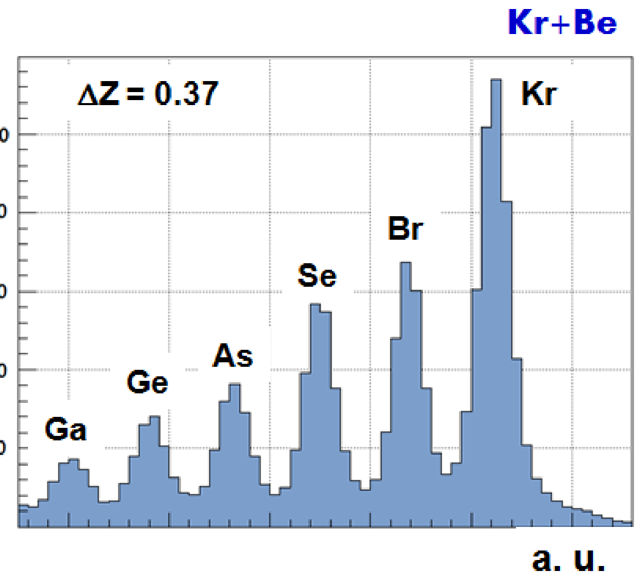


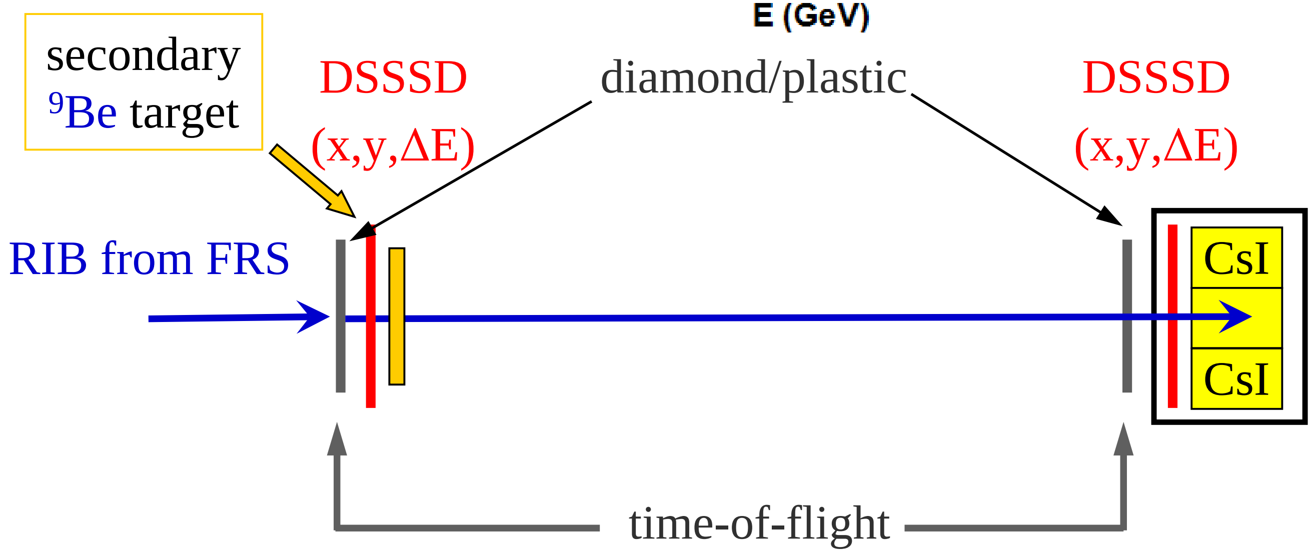


exp. observables:
**Z**, A, **θ**

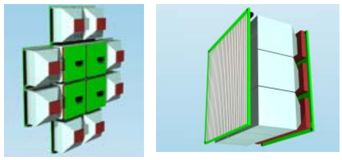

# Scattering experiment at relativistic energies

$$m \cdot c^2 = \frac{E_{kin}}{\gamma - 1}$$

with $E_{kin} = E_{CsI} + \Delta E_{DSSSD}$

and $\gamma = \frac{1}{\sqrt{1-\left(\frac{v}{c}\right)^2}}$

with v from LYCCA-ToF

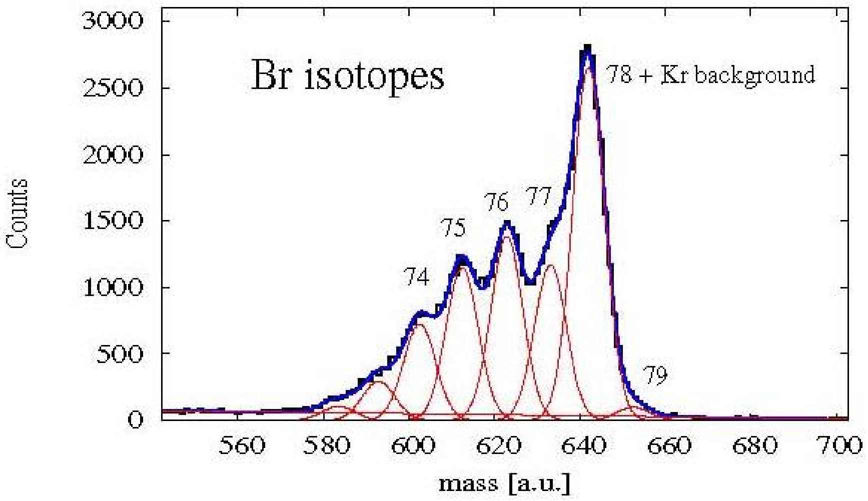


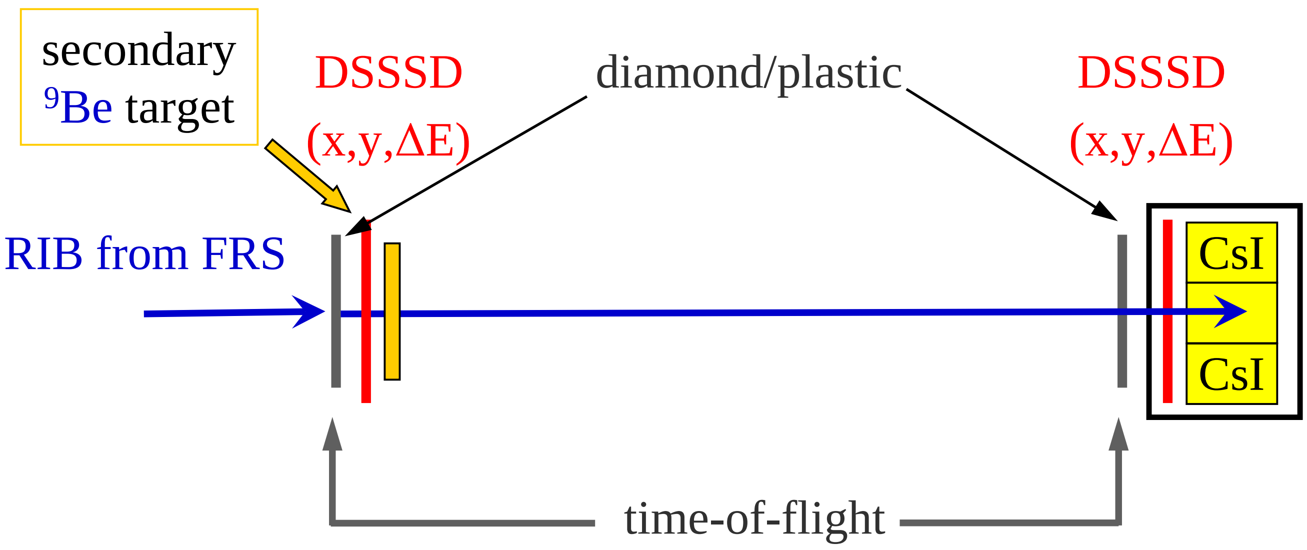


exp. observables:
**Z, A, θ**

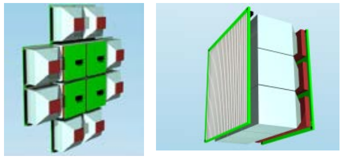

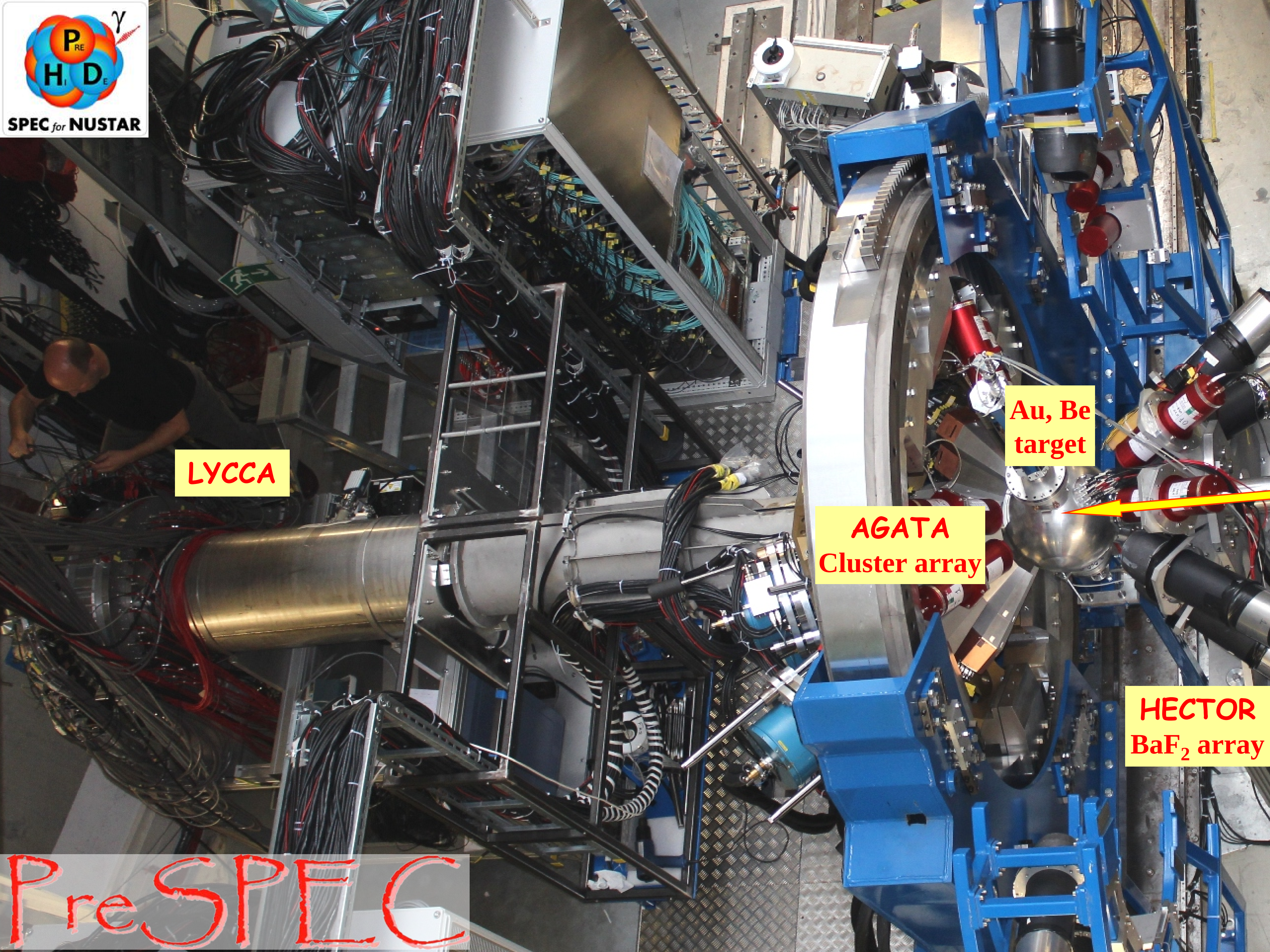
SPEC for NUSTAR
LYCCA
Au, Be target
AGATA Cluster array
HECTOR BaF$_2$ array
PreSPEC

# Lund-York-Cologne CAlorimeter

LUND UNIVERSITY | THE UNIVERSITY of York | University of Cologne

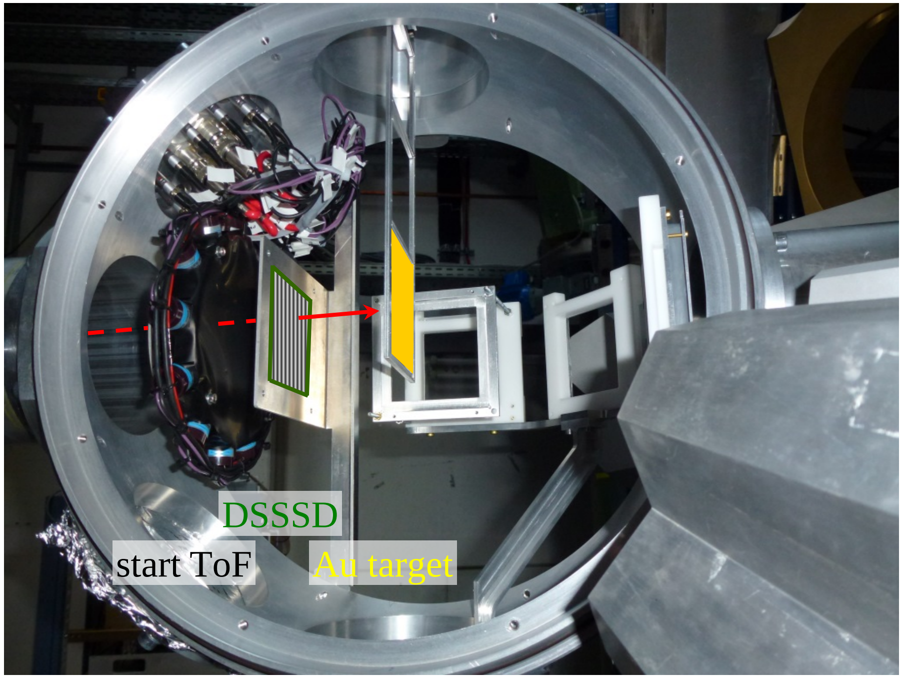


*PreSPEC target chamber*

***variable target position*** (13cm, 23cm)

*Pavel Golubev*

# Additional γ–ray background radiation

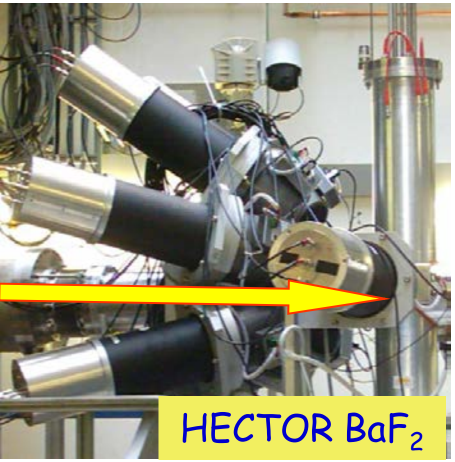


**$^{37}$Ca beam**
**at 196 MeV/u**

***Coulomb excitation:***
A/Q - $^{37}$Ca
all Ca detected in **ΔE-E**

1‰ interaction target
most γ-rays from CATE or LYCCA

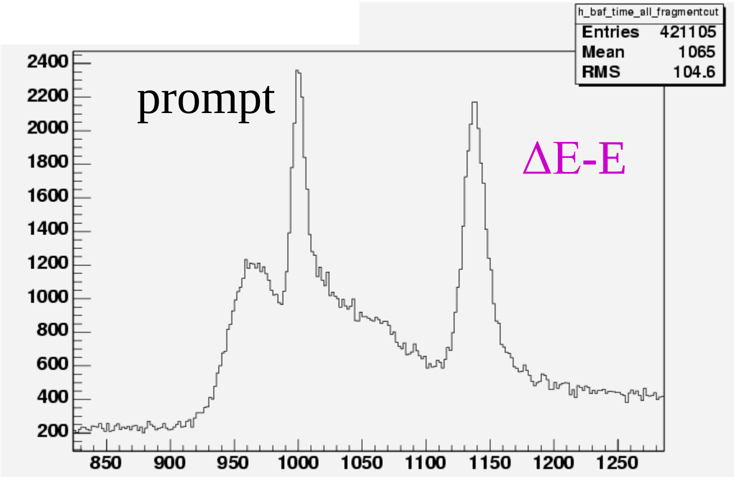


time spectrum

***Fragmentation:***
A/Q - $^{37}$Ca
K detected (mainly $^{36}$K)

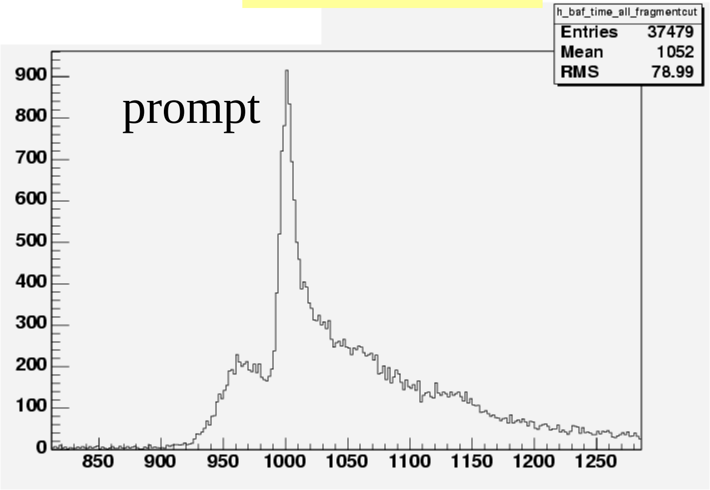

# Coulomb excitation of exotic nuclei

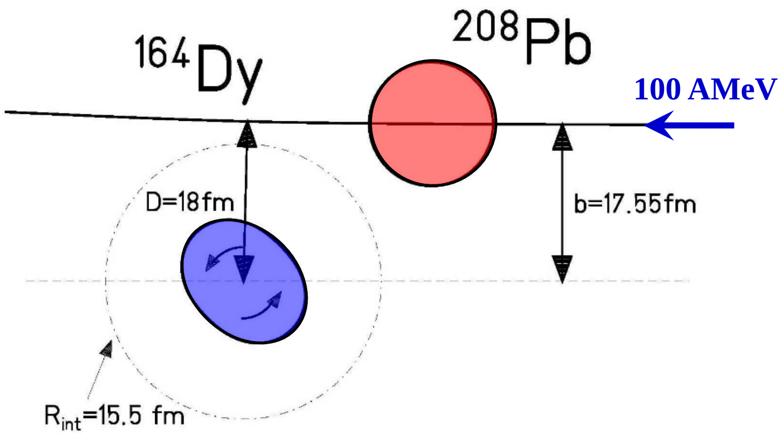


Electromagnetic interaction acting between two colliding nuclei.

- Inelastic scattering: kinetic energy is transferred into nuclear excitation energy
- Monopole-multipole interaction
- Target and projectile excitation possible

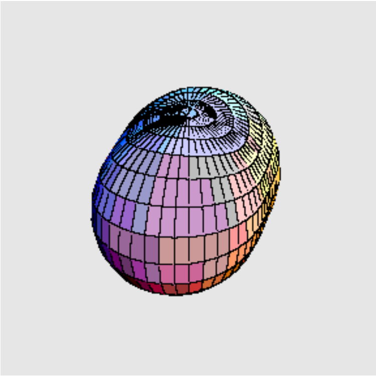

Excitation probability (or inelastic cross section) is a measure of the collectivity of the nuclear state of interest

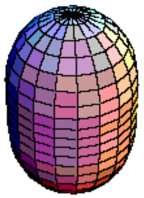

# Safe bombarding energy requirement – basic concept

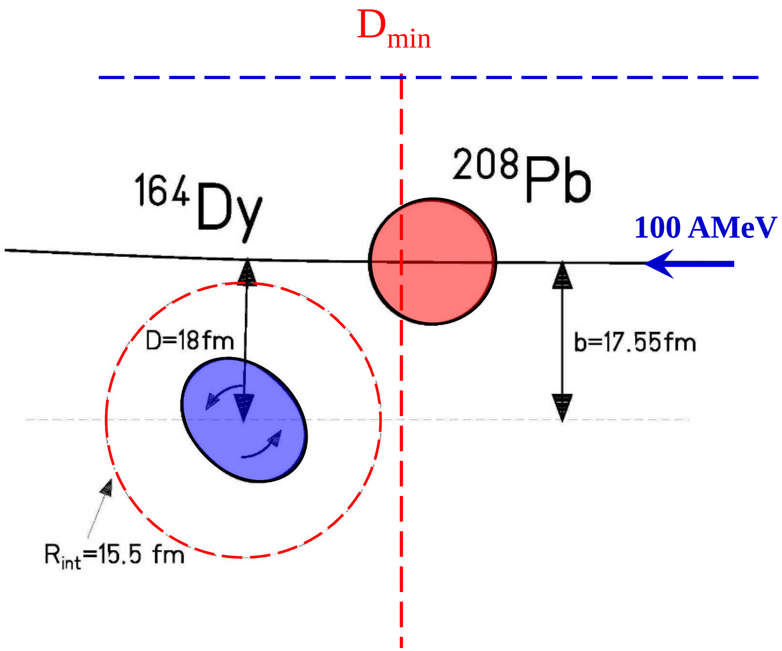


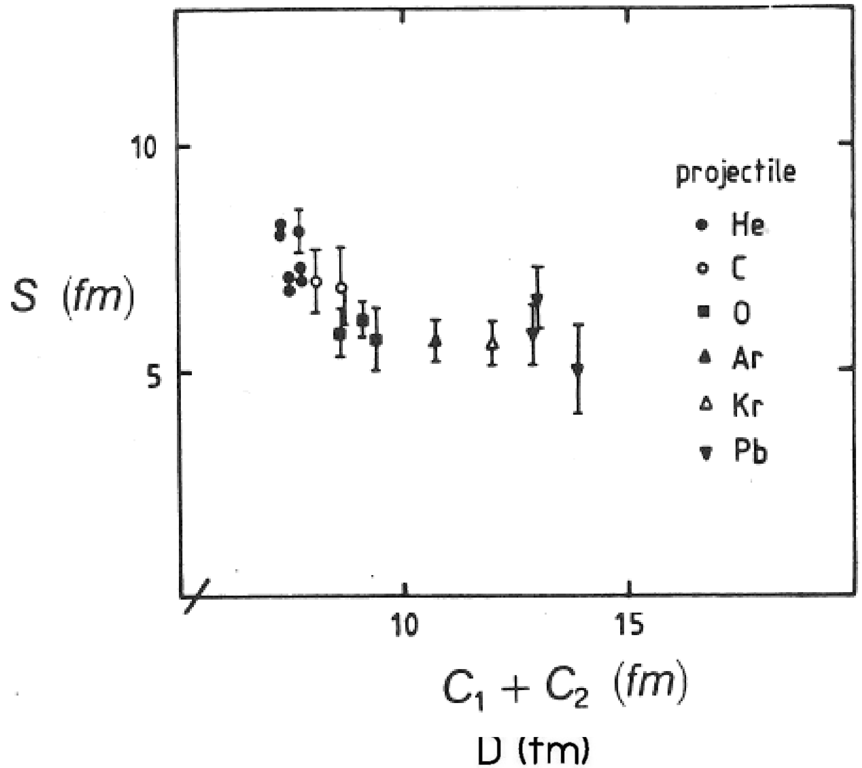


Rutherford scattering only if $D_{min}$ is large compared to nuclear radii + surfaces:

$$D_{\min} > C_P + C_T + 5 \ fm$$

$C_P$, $C_T$ half-density radii

➔ choose adequate beam energy ($D > D_{min}$ for all $\theta$)
low-energy Coulomb excitation

➔ limit scattering angle, i.e. select impact parameter $b > D_{min}$
high-energy Coulomb excitation

# High-energy Coulomb excitation – straight line approximation

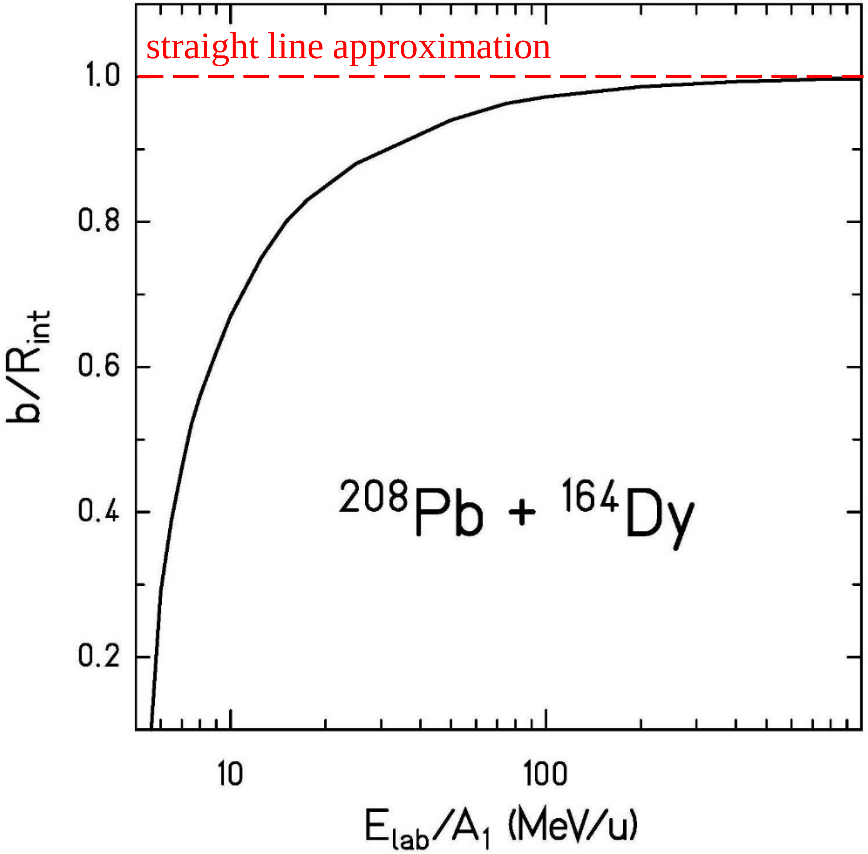


- distance of closest approach: $D(\theta_{cm}) = \frac{a}{\gamma} \cdot \left[1 + \sin^{-1}\left(\frac{\theta_{cm}}{2}\right)\right]$
- impact parameter: $\mathbf{b} = \frac{a}{\gamma} \cot\left(\frac{\theta_{cm}}{2}\right)$ ; $\mathbf{b} = \sqrt{D^2 - \frac{2 Z_P Z_T e^2}{m_0 c^2 \beta^2 \gamma} \cdot D}$
- straight line for large $E_{cm}$: b = D

zero degree detector

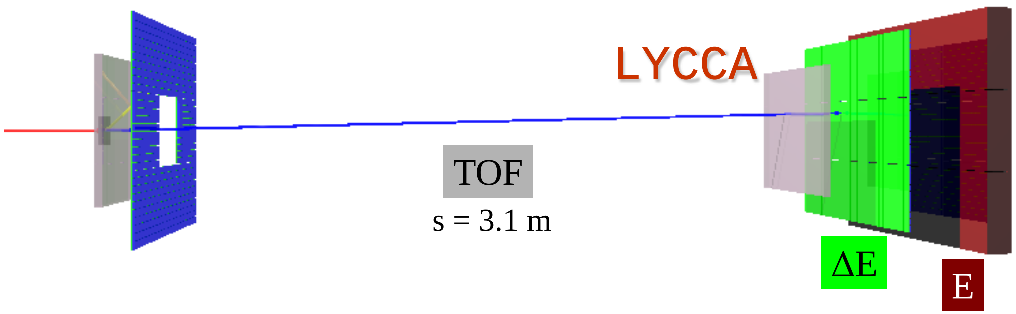


**L**und **Y**ork **C**ologne **CA**lorimeter

# High-energy Coulomb excitation – grazing angle and angular coverage of LYCCA

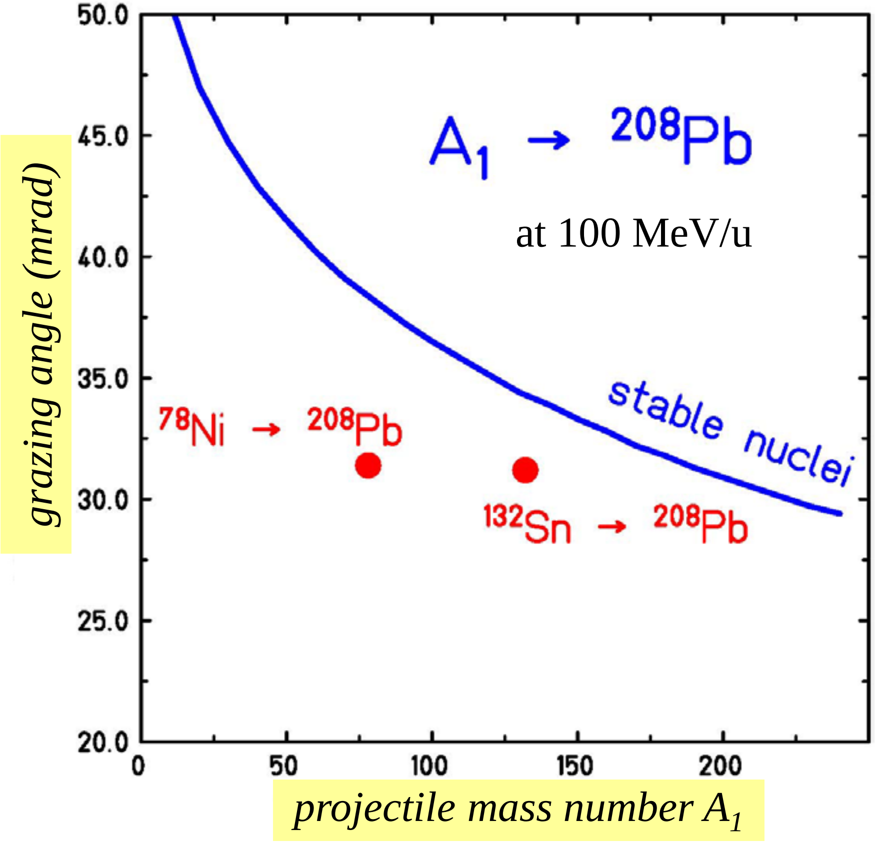


- distance of closest approach: $D(\theta_{cm}) = \frac{a}{\gamma} \cdot \left[1 + \sin^{-1}\left(\frac{\theta_{cm}}{2}\right)\right]$

For nonrelativistic projectiles:

$$2 \cdot \sin\left(\frac{\theta_{1/4}}{2}\right) = \frac{a}{R_{int} - a} \quad with \quad a = \frac{Z_P Z_T e^2}{m_0 c^2 \beta^2 \gamma}$$

For relativistic projectiles ($\theta_{cm} \approx \vartheta_{lab}$):

$$\vartheta_{1/4} = \frac{2 \cdot Z_P Z_T e^2}{m_0 c^2 \beta^2 \gamma} \cdot \frac{1}{R_{int}}$$

*Coulomb excitation:* $\vartheta_1^{lab} < \vartheta_{1/4}$

# High-energy Coulomb excitation – grazing angle

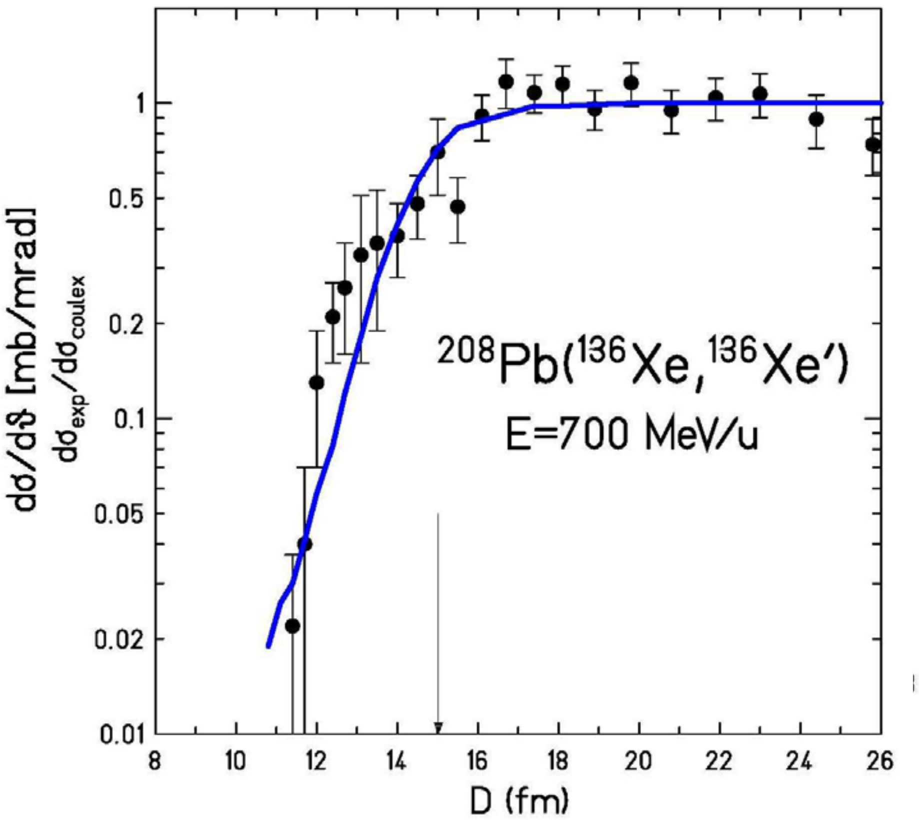


$^{136}$Xe on $^{208}$Pb at 700 MeV/u

*excitation of giant dipole resonance*

$R_{\text{int}} = 15.0\ fm \ \rightarrow\ \vartheta_{1/4} = 5.7\, mrad$

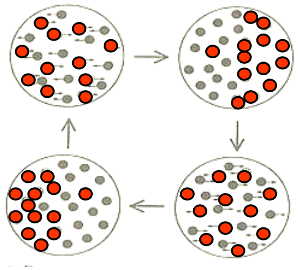


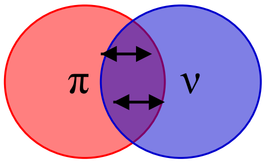


For relativistic projectiles ($\theta_{cm} \approx \vartheta_{lab}$):

$$D = \frac{2 \cdot Z_P Z_T e^2}{m_0 c^2 \beta^2 \gamma} \cdot \frac{1}{\vartheta}$$

A.Grünschloß et al., Phys. Rev. C60 051601 (1999)

# Scattering experiments at relativistic energies

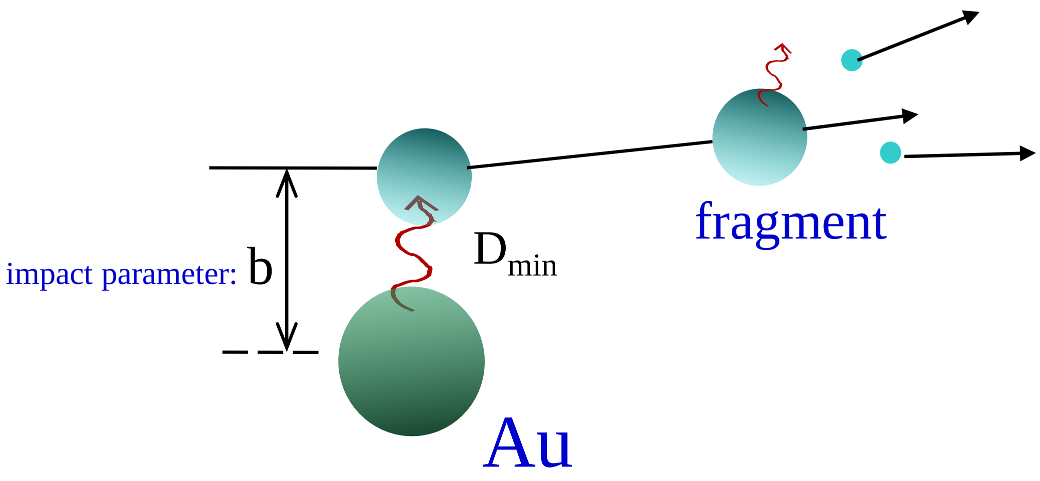


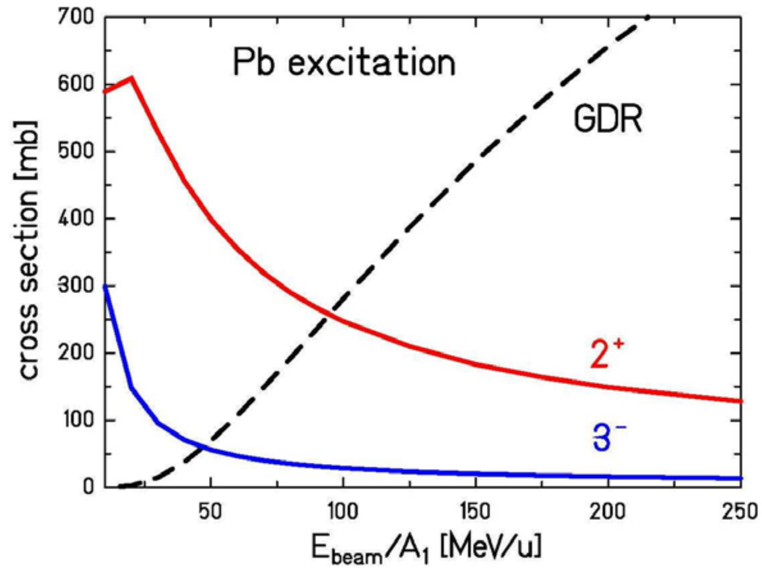


Rutherford scattering only if distance of closest approach $D_{min}$ is large compared to nuclear radii + surfaces:

$$D_{min} > C_P + C_T + 5\ fm$$

$C_P$, $C_T$ half-density radii

$$\sigma_{\pi\lambda} \approx \left(\frac{Z_P e^2}{\hbar c}\right)^2 \cdot \frac{\pi}{e^2 b^{2\lambda-2}} \cdot B(\pi\lambda;0\to\lambda) \cdot \begin{cases} (\lambda-1)^{-1} & for\ \ \lambda \geq 2 \\ 2\ln(b_a/b) & for\ \ \lambda = 1 \end{cases}$$

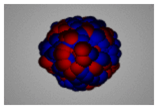

$E^* \cong 13.3\,MeV$

$B(E1;0\to 1^-) \cong 0.55\,e^2 b$

$E^* = 4.086\,MeV$

$B(E2;0\to 2^+) = 9\,Wu$

$E^* = 2.615\,MeV$

$B(E3;0\to 3^-) = 34\,Wu$

# High-energy Coulomb excitation – M1 and E2 excitations, full analytical description

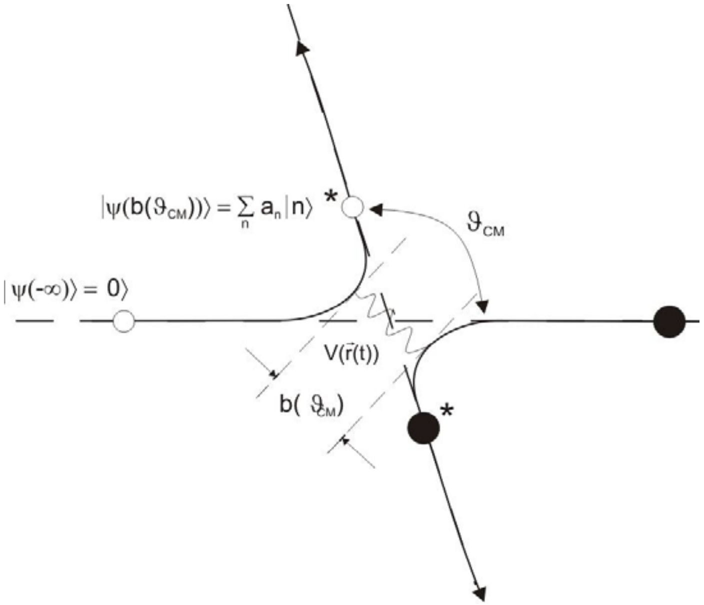


The scattering of a nucleus $^{A_P}_{Z_P}X_{N_P}$ on a target nucleus $^{A_T}_{Z_T}Y_{N_T}$

$$\sigma_{E\lambda} = \left(\frac{Z_1 e}{\hbar v}\right)^2 a^{-2\lambda+2} B(E\lambda, I_0 \to I_f)\, f_{E\lambda}(\xi)$$

$$\sigma_{M\lambda} = \left(\frac{Z_1 e}{\hbar c}\right)^2 a^{-2\lambda+2} B(M\lambda, I_0 \to I_f)\, f_{M\lambda}(\xi)$$

$$\frac{\sigma_{E\lambda}}{\sigma_{M\lambda}} \sim \left(\frac{c}{v}\right)^2; \quad v/c \sim 7\% \to \frac{\sigma_{E\lambda}}{\sigma_{M\lambda}} \sim 200$$

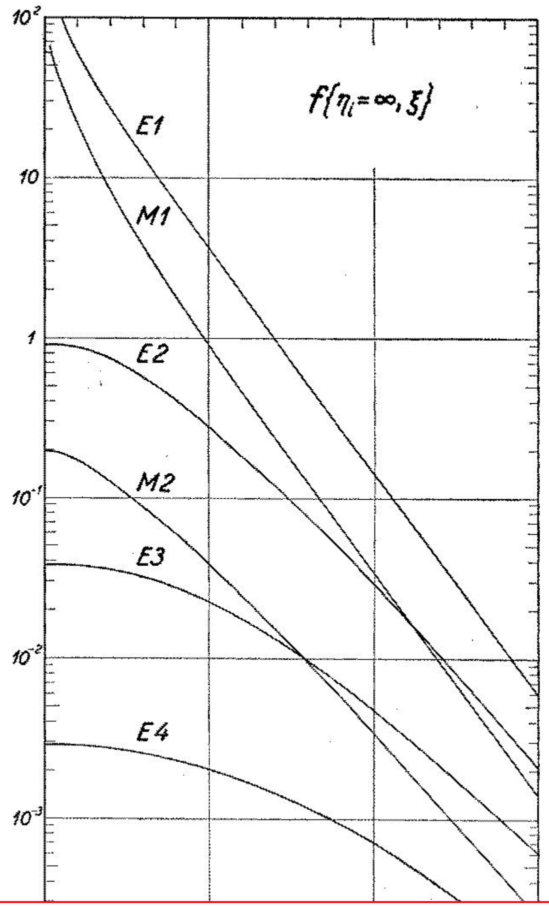


***Conclusion:***

1) The lower multipolarities are dominant
2) For a given multipole order, electric transitions are more likely than magnetic transitions

# High-energy Coulomb excitation – M1 and E2 excitations

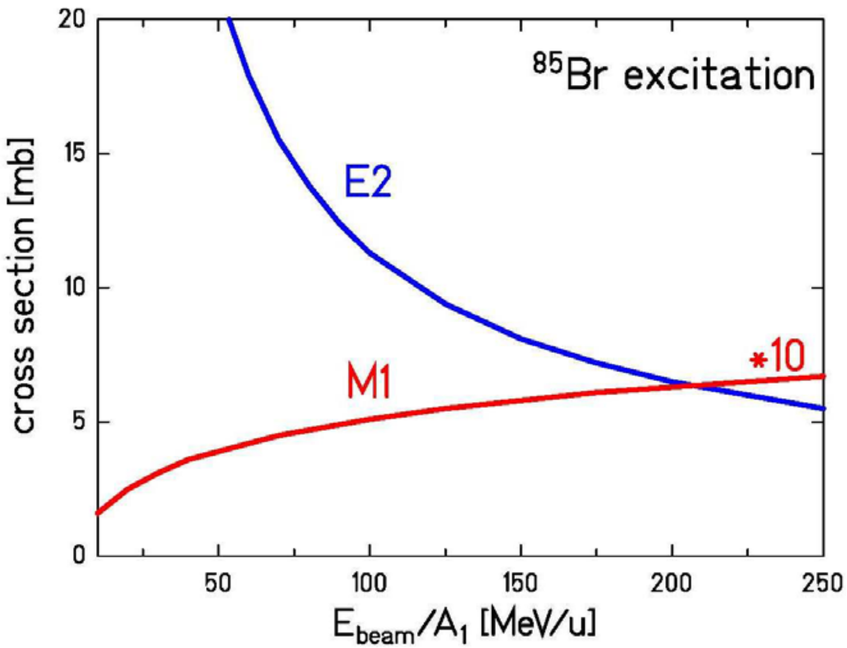


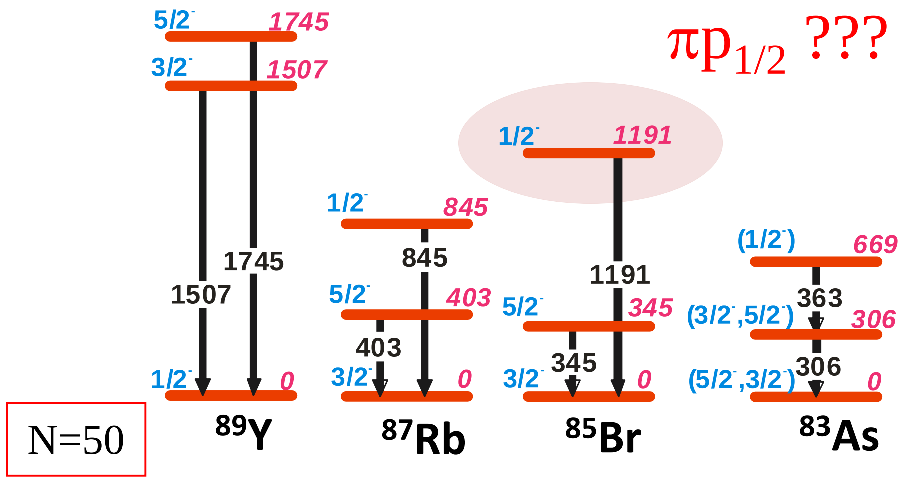


$\pi p_{1/2}$ ???

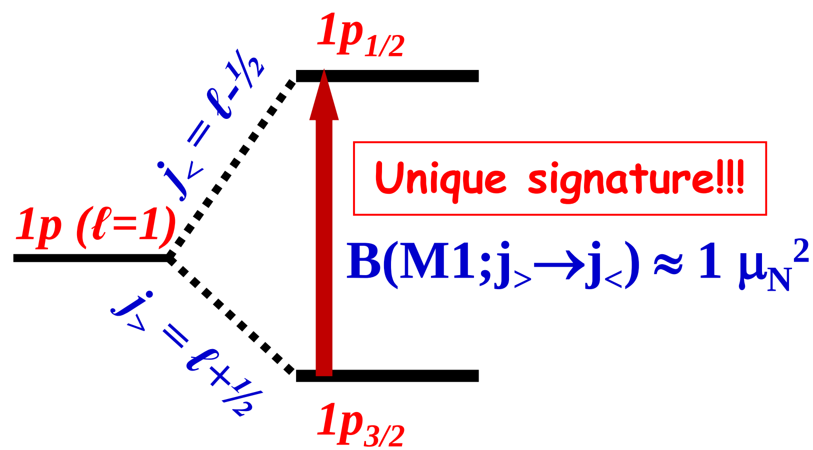


$^{85}$Br $\rightarrow$ $^{197}$Au at 100 MeV/u

rate = $10^5\ s^{-1} \cdot 10^{21}\ cm^{-2} \cdot 0.5 \cdot 10^{-27}\ cm^2 \cdot 10\% = 22\ h^{-1}$

# Scattering experiments at relativistic energies

Doppler effect:

$$\frac{E_{\gamma 0}}{E_\gamma} = \frac{1 - \beta \cdot cos\vartheta_\gamma^{lab}}{\sqrt{1-\beta^2}} \quad \text{for } \vartheta_p \cong 0^0$$

Lorentz boost:

$$\frac{d\Omega_{rest}}{d\Omega_{lab}} = \left(\frac{E_\gamma}{E_{\gamma 0}}\right)^2$$

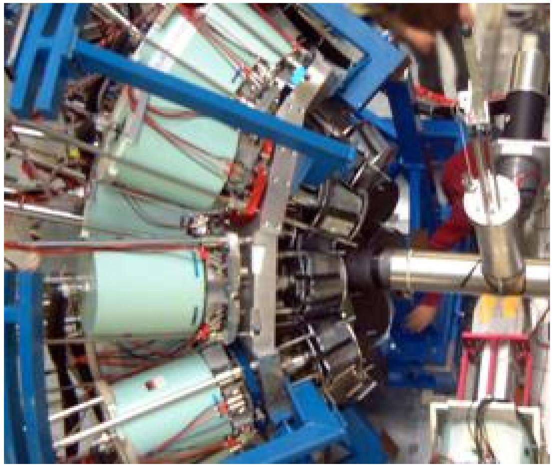


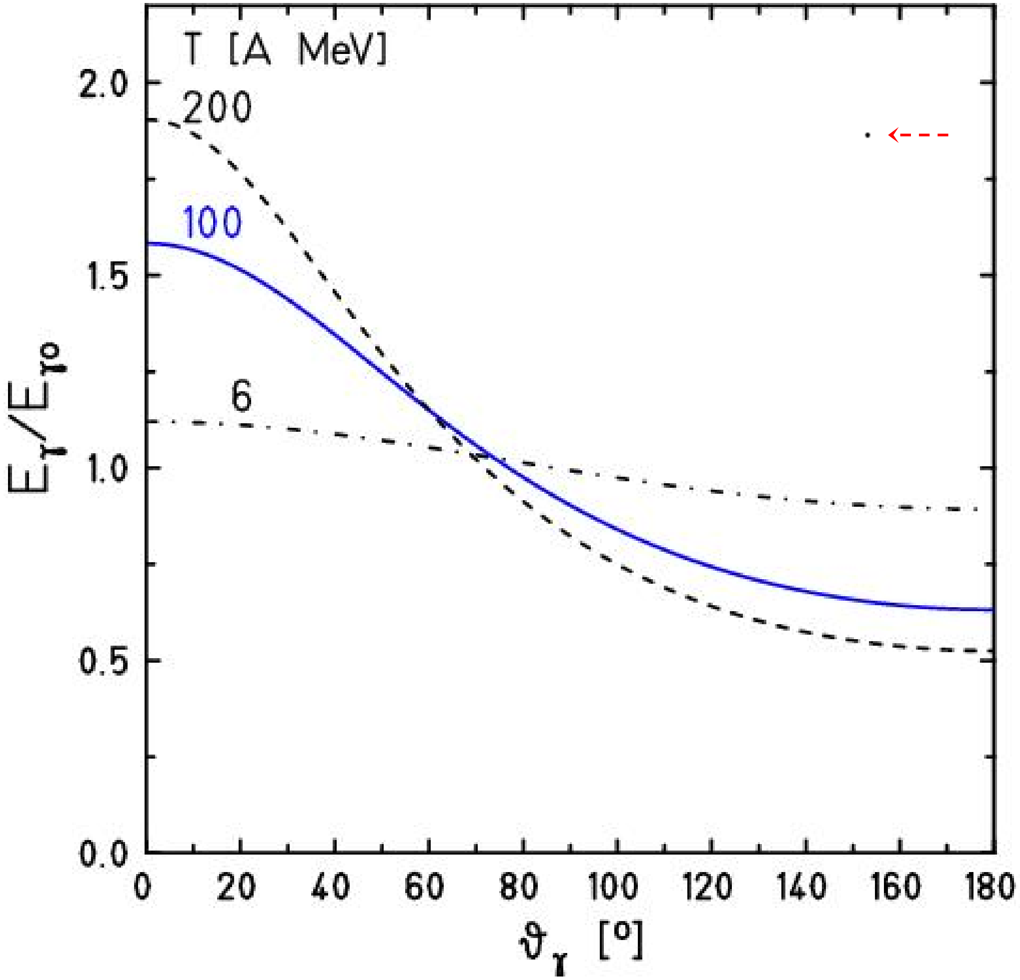

# Doppler-shift correction – $^{238}$U on $^{197}$Au (386 mg/cm$^2$) at 183 AMeV

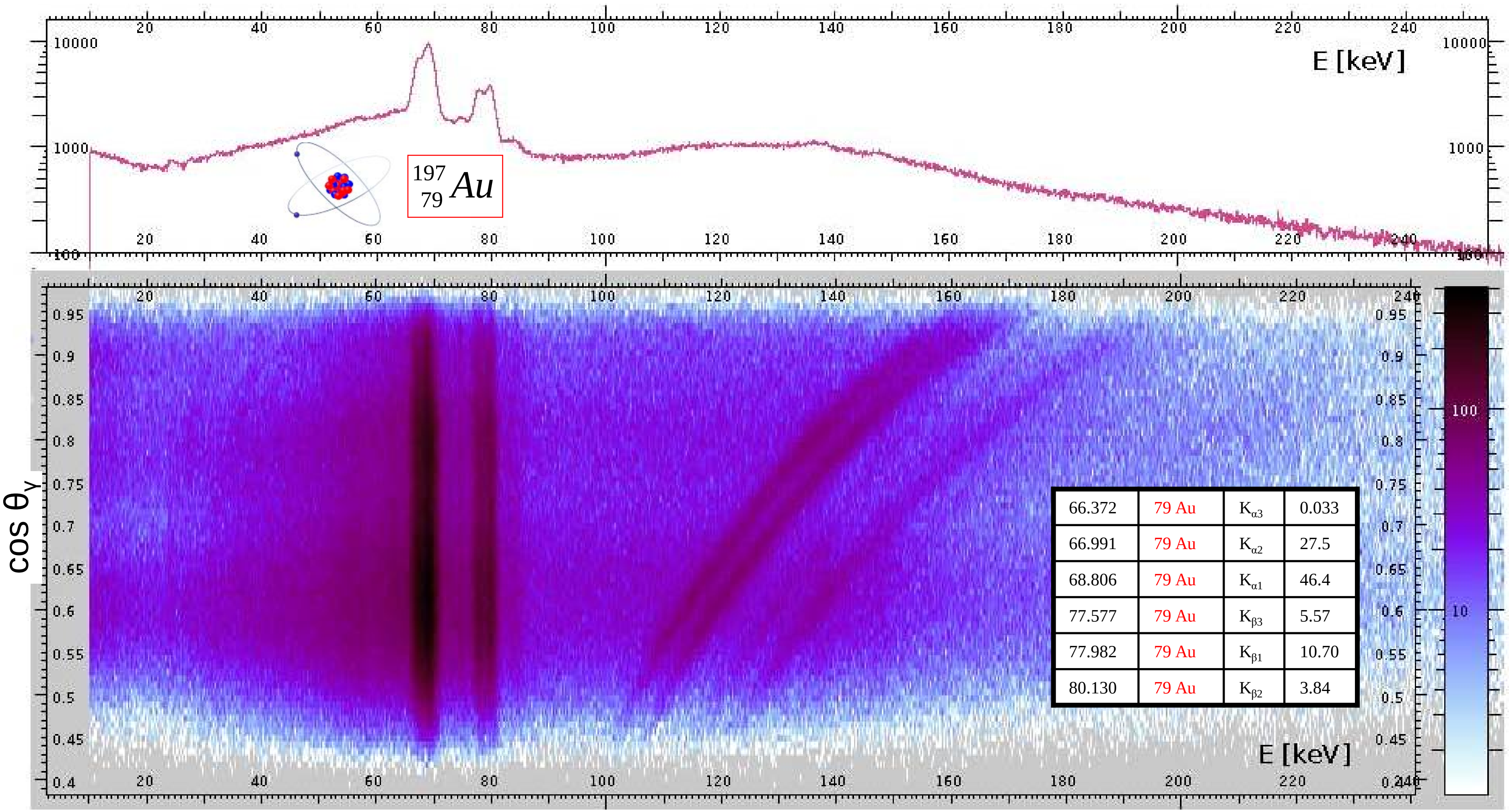


| | | | |
|---|---|---|---|
| 66.372 | 79 Au | $K_{\alpha3}$ | 0.033 |
| 66.991 | 79 Au | $K_{\alpha2}$ | 27.5 |
| 68.806 | 79 Au | $K_{\alpha1}$ | 46.4 |
| 77.577 | 79 Au | $K_{\beta3}$ | 5.57 |
| 77.982 | 79 Au | $K_{\beta1}$ | 10.70 |
| 80.130 | 79 Au | $K_{\beta2}$ | 3.84 |

http://ie.lbl.gov/atomic/x2.pdf

*Michael Reese*

# Doppler-shift correction – $^{238}$U on $^{197}$Au (386 mg/cm$^2$) at 183 AMeV

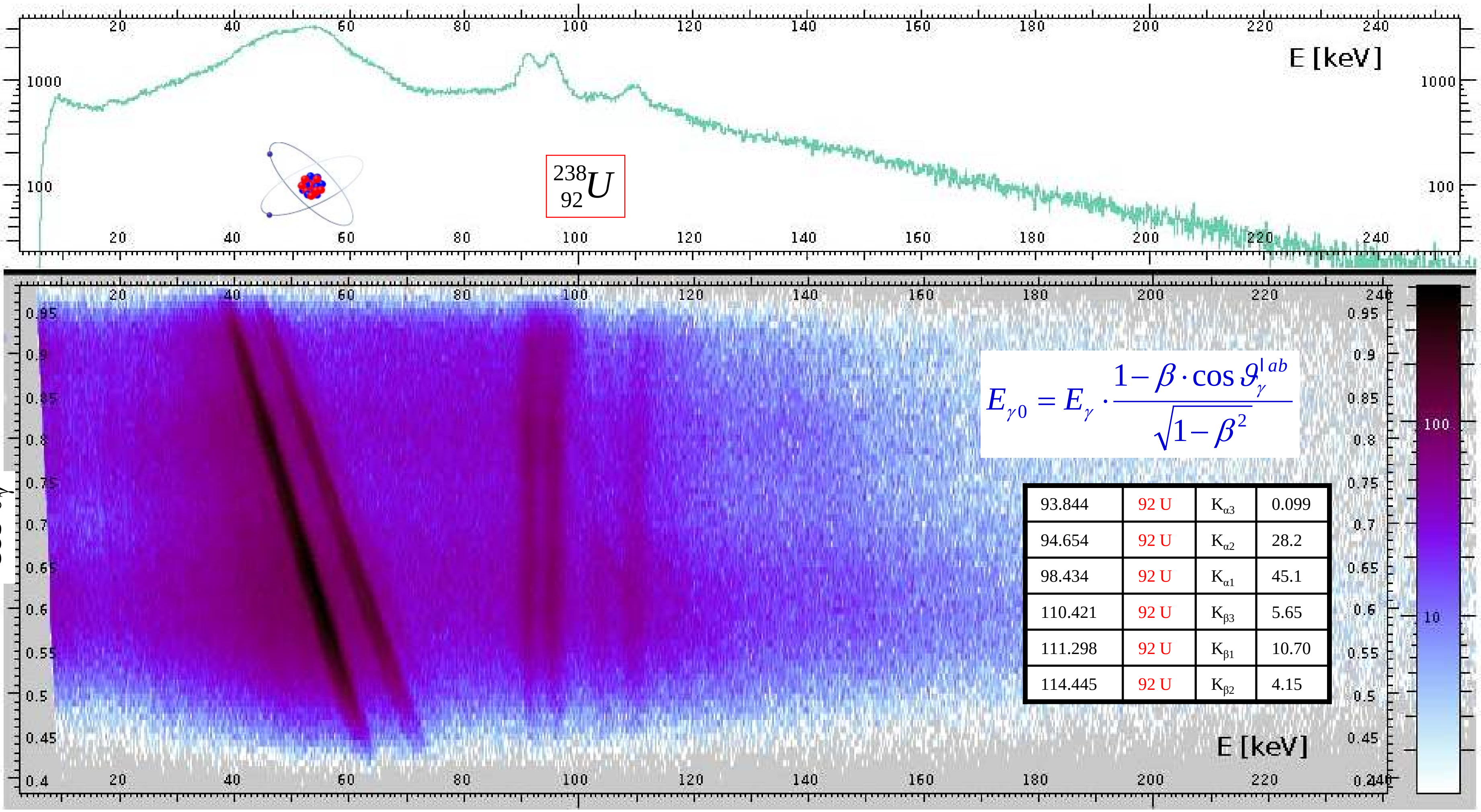


$$E_{\gamma 0} = E_\gamma \cdot \frac{1-\beta\cdot\cos\vartheta_\gamma^{lab}}{\sqrt{1-\beta^2}}$$

| | | | |
|---|---|---|---|
| 93.844 | 92 U | $K_{\alpha 3}$ | 0.099 |
| 94.654 | 92 U | $K_{\alpha 2}$ | 28.2 |
| 98.434 | 92 U | $K_{\alpha 1}$ | 45.1 |
| 110.421 | 92 U | $K_{\beta 3}$ | 5.65 |
| 111.298 | 92 U | $K_{\beta 1}$ | 10.70 |
| 114.445 | 92 U | $K_{\beta 2}$ | 4.15 |

http://ie.lbl.gov/atomic/x2.pdf

*Michael Reese*

# Doppler broadening and position resolution

$$E_{\gamma 0} = E_{\gamma}\frac{1-\beta\cdot\cos\vartheta_{\gamma}}{\sqrt{1-\beta^{2}}} \qquad \left(\beta,\ \vartheta_{p}=0^{0},\ \vartheta_{\gamma}\ \text{and}\ E_{\gamma}\ \text{in lab}-\text{frame}\right)$$

$$\left(\frac{\Delta E_{\gamma 0}}{E_{\gamma 0}}\right)^{2} = \left(\frac{\beta\cdot\sin\vartheta_{\gamma}}{1-\beta\cdot\cos\vartheta_{\gamma}}\right)^{2}\left(\Delta\vartheta_{\gamma}\right)^{2} + \left(\frac{\beta-\cos\vartheta_{\gamma}}{\left(1-\beta^{2}\right)\cdot\left(1-\beta\cdot\cos\vartheta_{\gamma}\right)}\right)^{2}\left(\Delta\beta\right)^{2} + \left(\frac{1}{E_{\gamma}}\right)^{2}\left(\Delta E_{\gamma}\right)^{2}$$

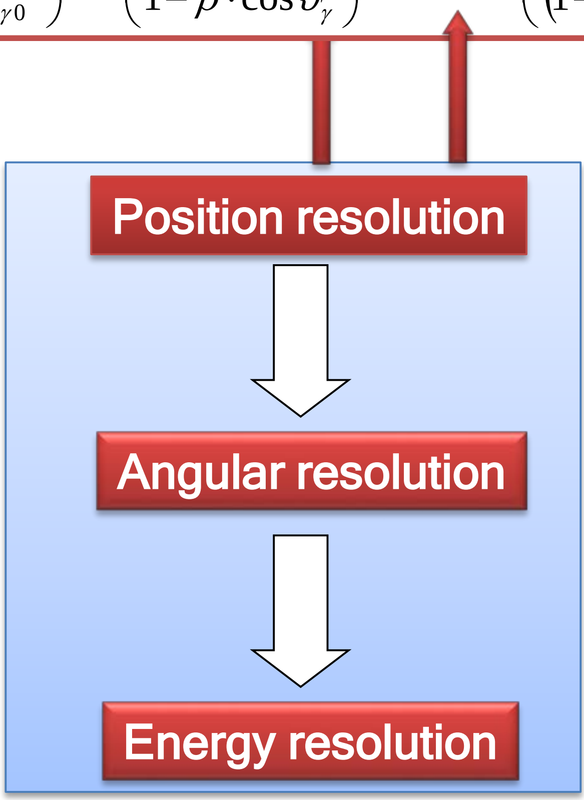


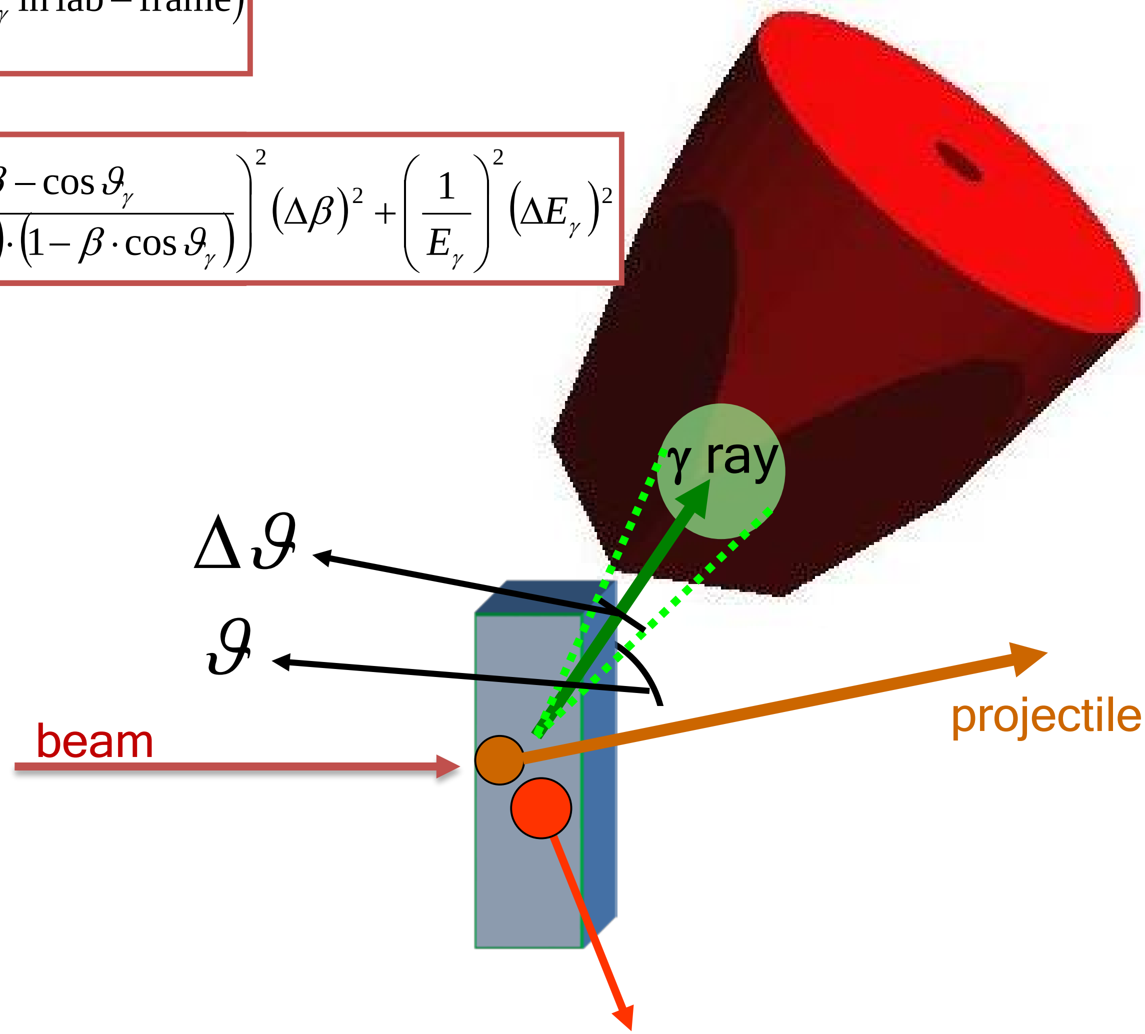

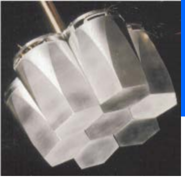

# Doppler broadening

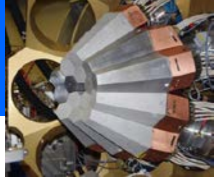

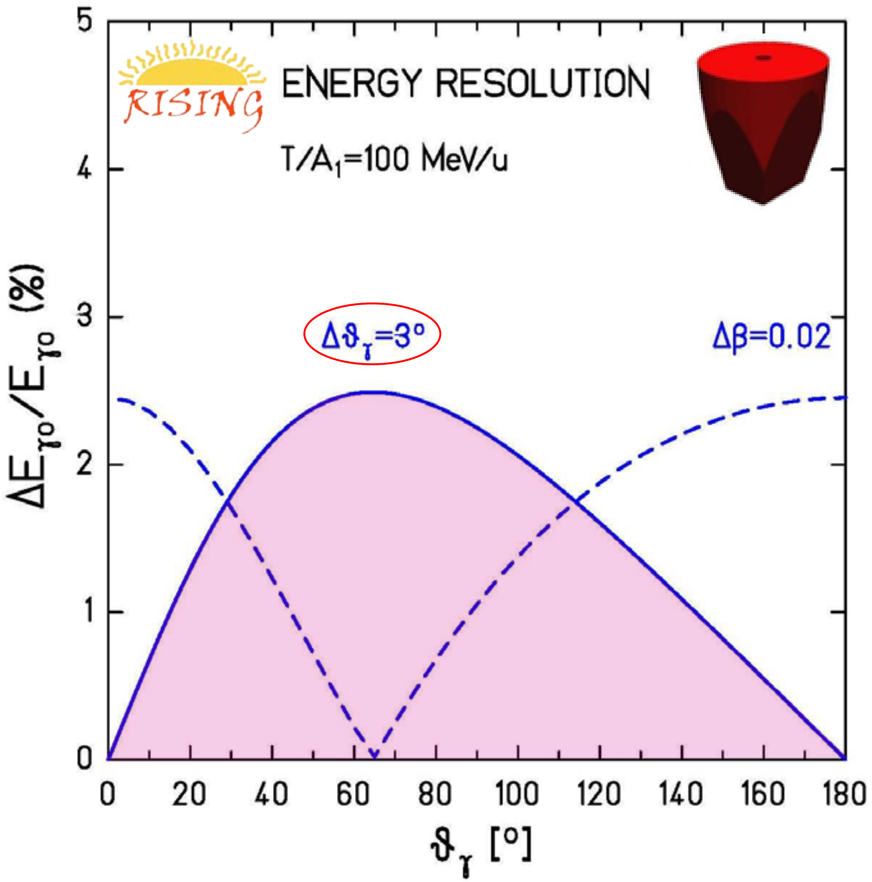


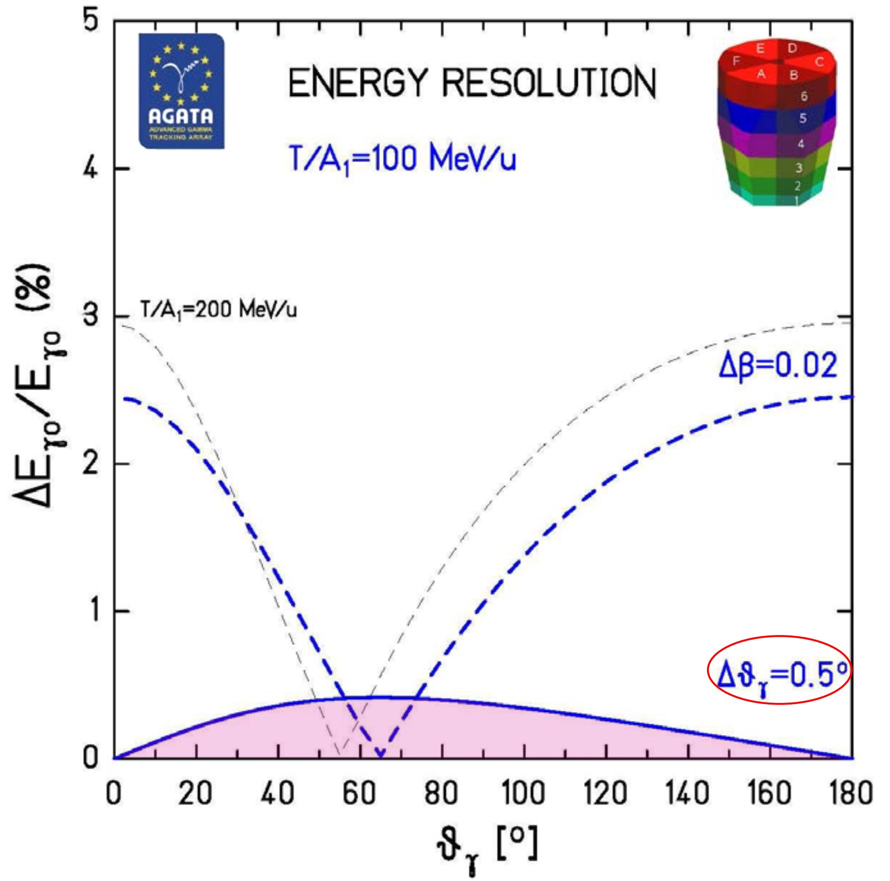


opening angle:

$$\frac{\Delta E_{\gamma 0}}{E_{\gamma 0}} = \frac{\beta \cdot \sin\vartheta_\gamma}{1-\beta\cdot\cos\vartheta_\gamma}\cdot\Delta\vartheta_\gamma$$

slowing down in target:

$$\frac{\Delta E_{\gamma 0}}{E_{\gamma 0}} = \frac{\beta - \cos\vartheta_\gamma}{\left(1-\beta^2\right)\cdot\left(1-\beta\cdot\cos\vartheta_\gamma\right)}\cdot\Delta\beta$$

# Segmented detectors

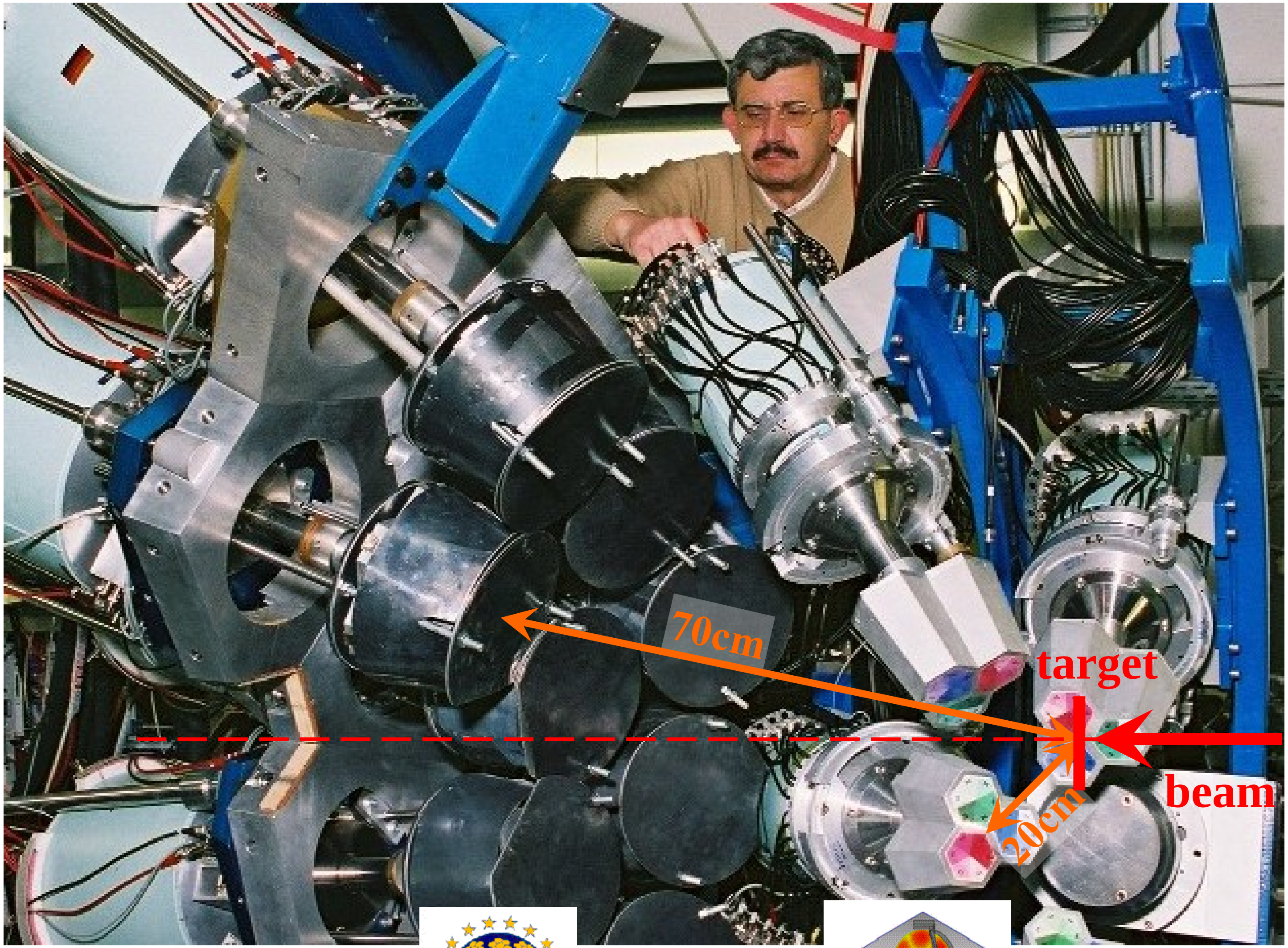

# Advanced GAmma Tracking Array

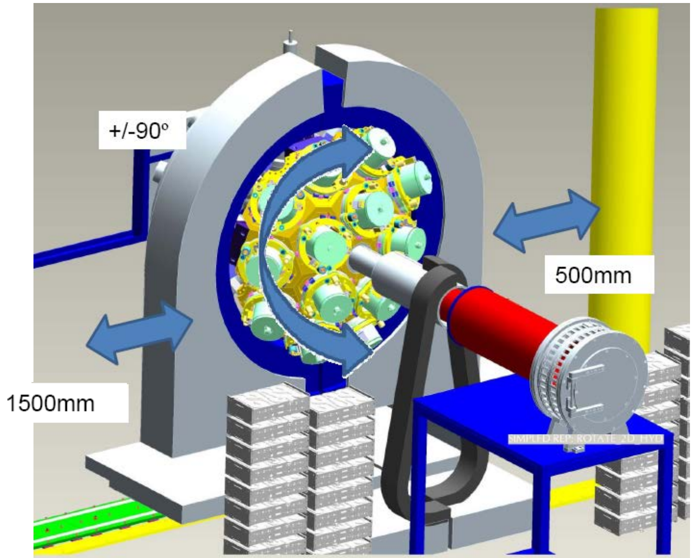


*John Strachan*

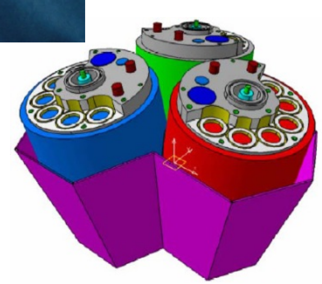

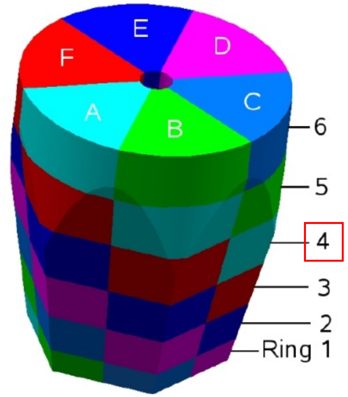


**Signals from 36 segments + core** are measured as a function of time (γ-ray interaction point)

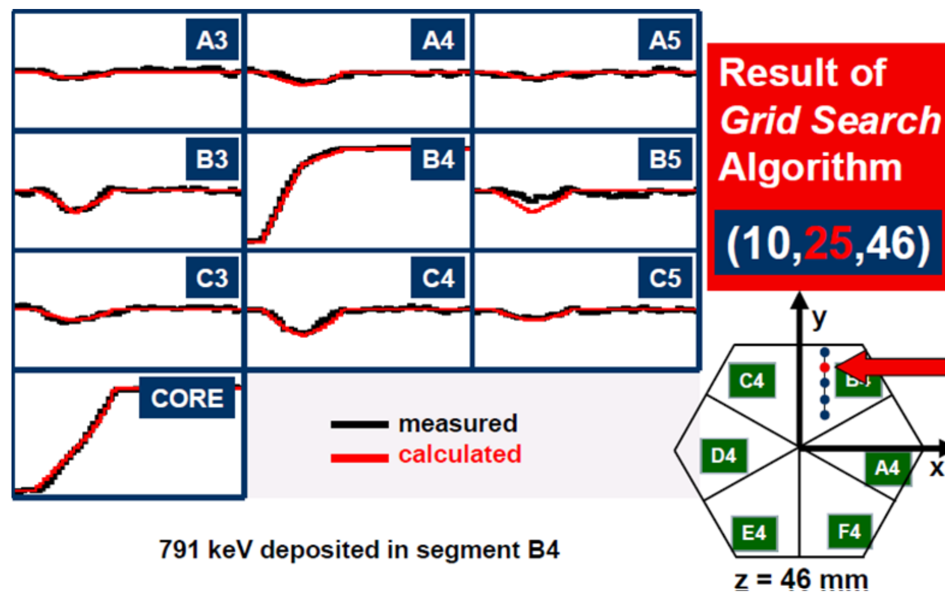

# Scattering experiment at relativistic energies

$^{80}$Kr $\longrightarrow$ $^{197}$Au, 150 AMeV

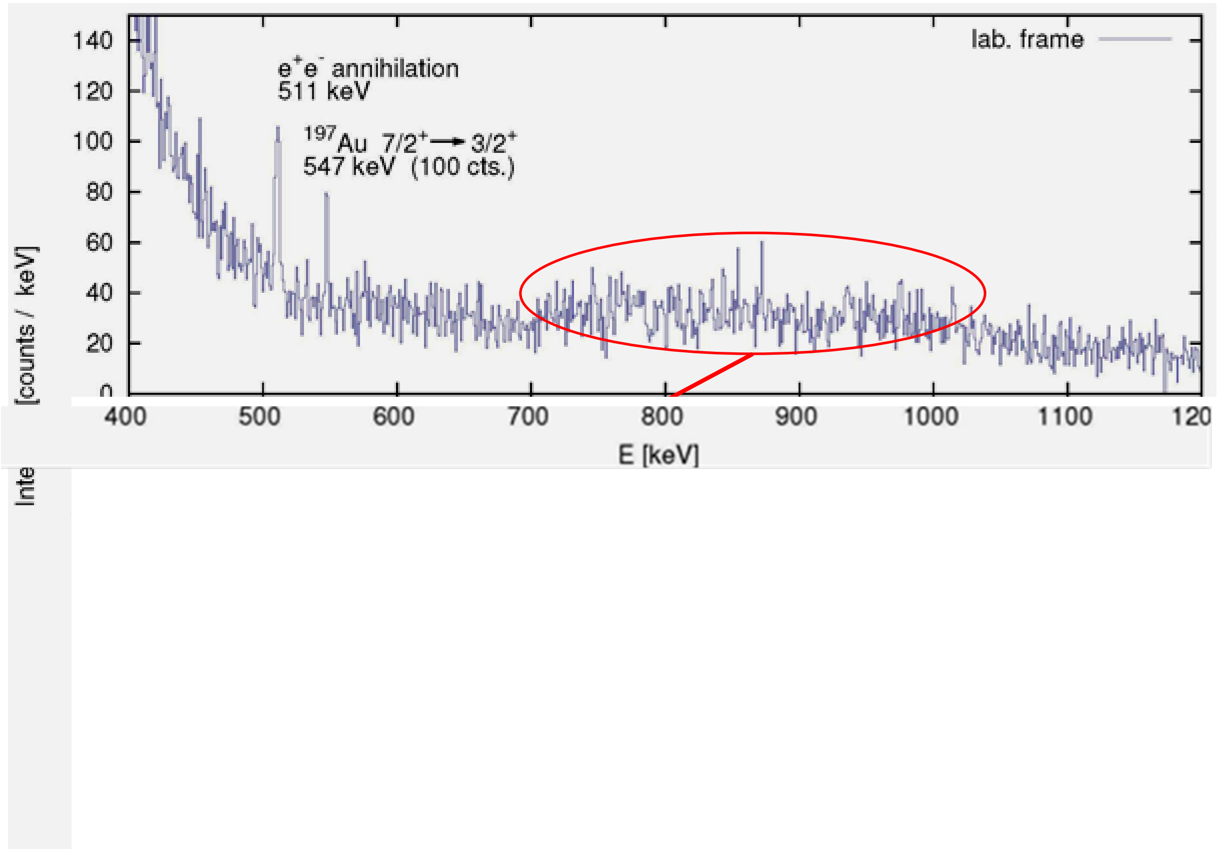


Doppler effect

$$\frac{E_{\gamma 0}}{E_{\gamma}} = \frac{1-\beta \cdot \cos \vartheta_{\gamma}^{lab}}{\sqrt{1-\beta^2}}$$

# High-energy Coulomb excitation – triaxiality in even-even nuclei (N=76)

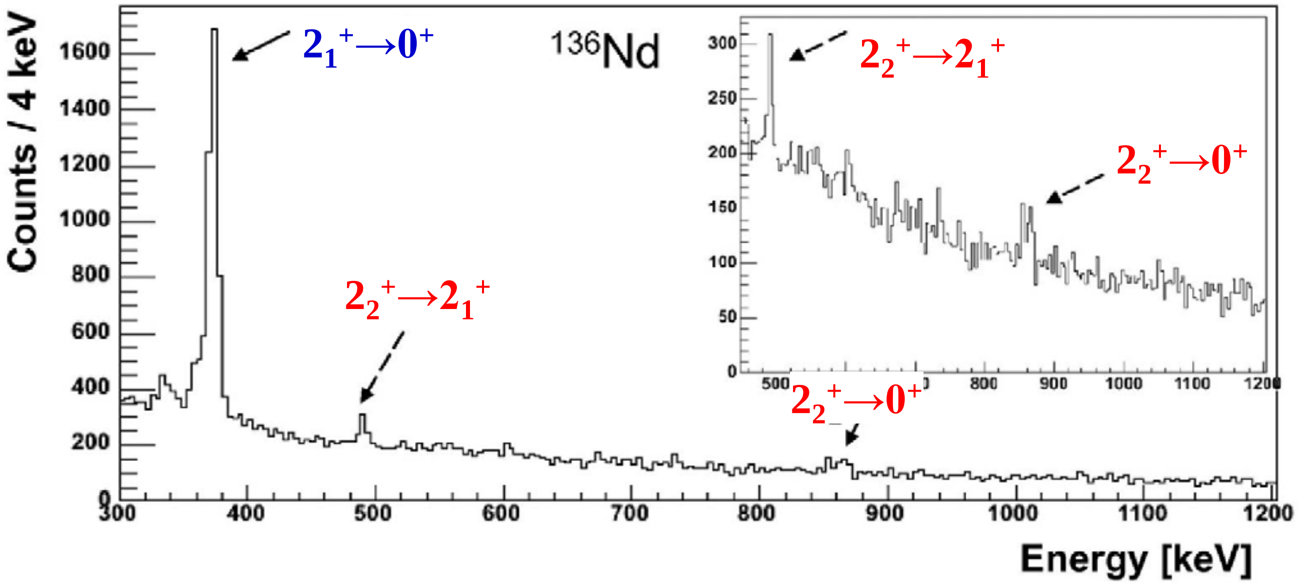


***First observation of a second excited 2$^+$ state***
populated in a Coulomb experiment at 100 AMeV using EUROBALL and MINIBALL Ge-detectors.

- ➢ shape symmetry
- ➢ collective strength

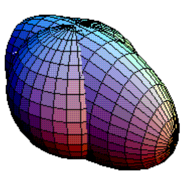

$$\frac{B(E2;2_2\rightarrow 2_1)}{B(E2;2_1\rightarrow 0)} = \frac{\frac{20}{7}\,\frac{\sin^2(3\gamma)}{9-8\sin^2(3\gamma)}}{1+\frac{3-2\sin^2(3\gamma)}{\sqrt{9-8\sin^2(3\gamma)}}}$$

$$\frac{B(E2;2_2\rightarrow 0)}{B(E2;2_1\rightarrow 0)} = \frac{1-\frac{3-2\sin^2(3\gamma)}{\sqrt{9-8\sin^2(3\gamma)}}}{1+\frac{3-2\sin^2(3\gamma)}{\sqrt{9-8\sin^2(3\gamma)}}}$$

$$\frac{E_2(2)}{E_1(2)} = \frac{3+\sqrt{9-8\sin^2 3\gamma}}{3-\sqrt{9-8\sin^2 3\gamma}}$$

T.R. Saito et al. Phys.Lett. B669 (2008), 19

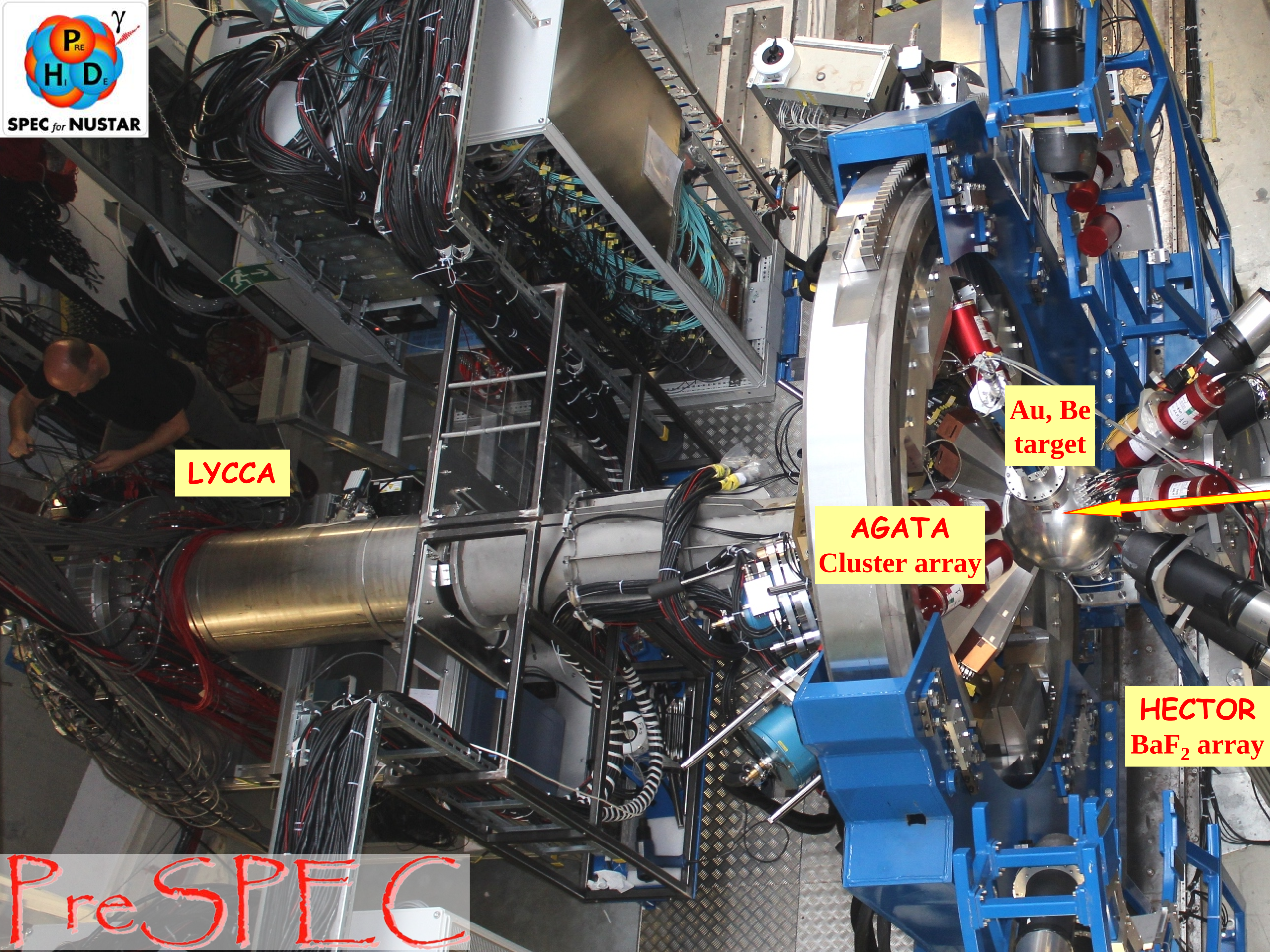
SPEC for NUSTAR
LYCCA
Au, Be
target
AGATA
Cluster array
HECTOR
BaF$_2$ array
PreSPEC

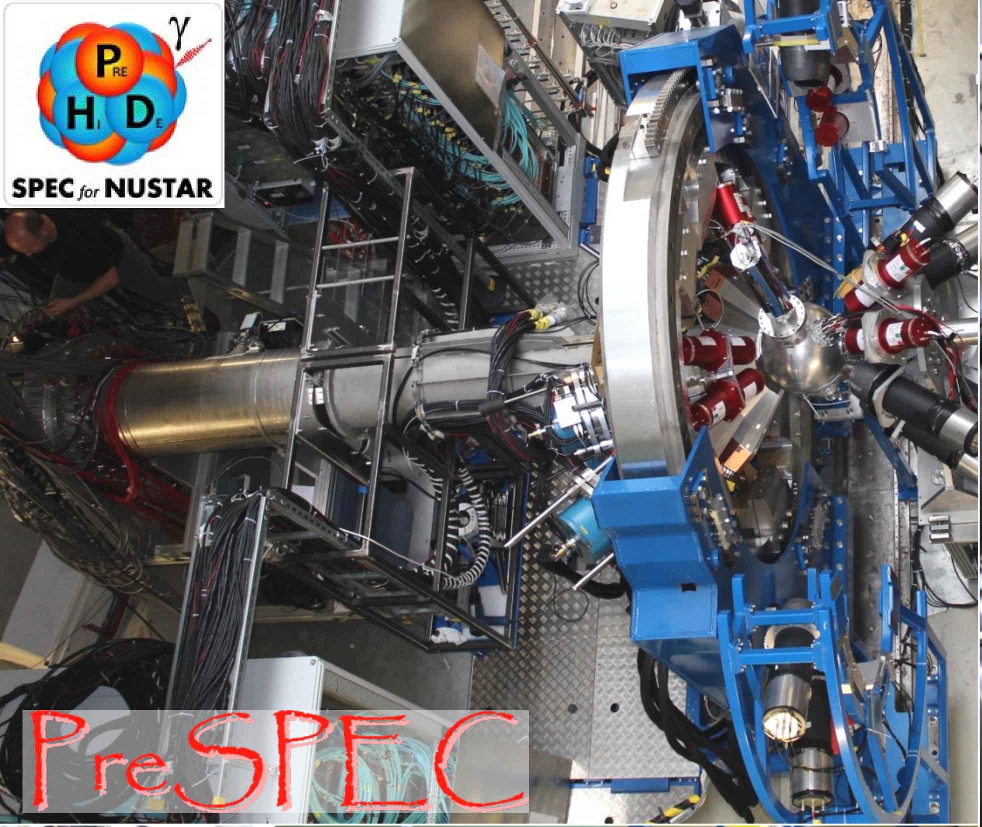
SPEC for NUSTAR
PreSPEC

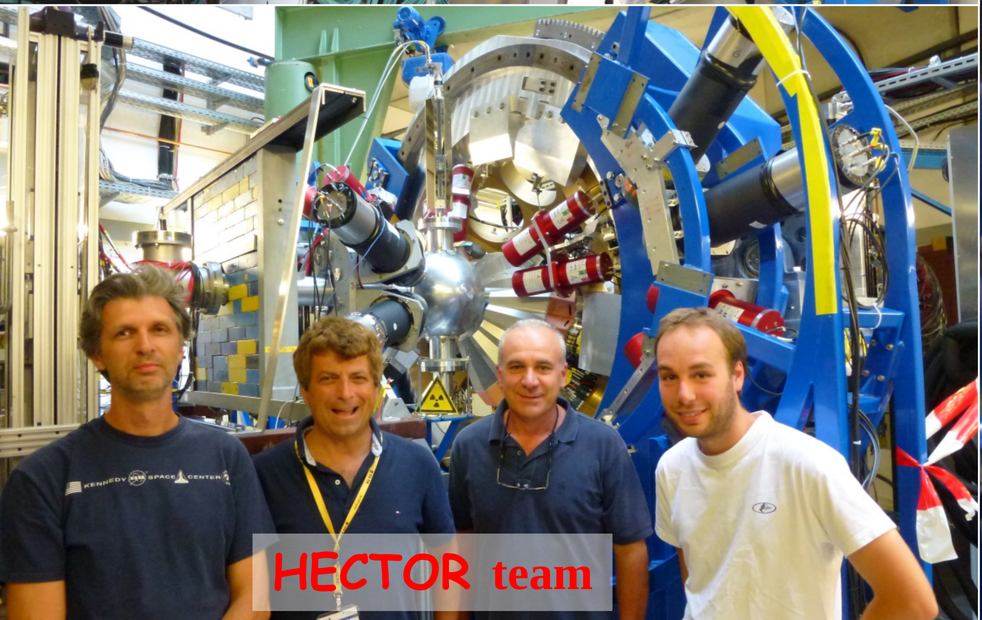
HECTOR team

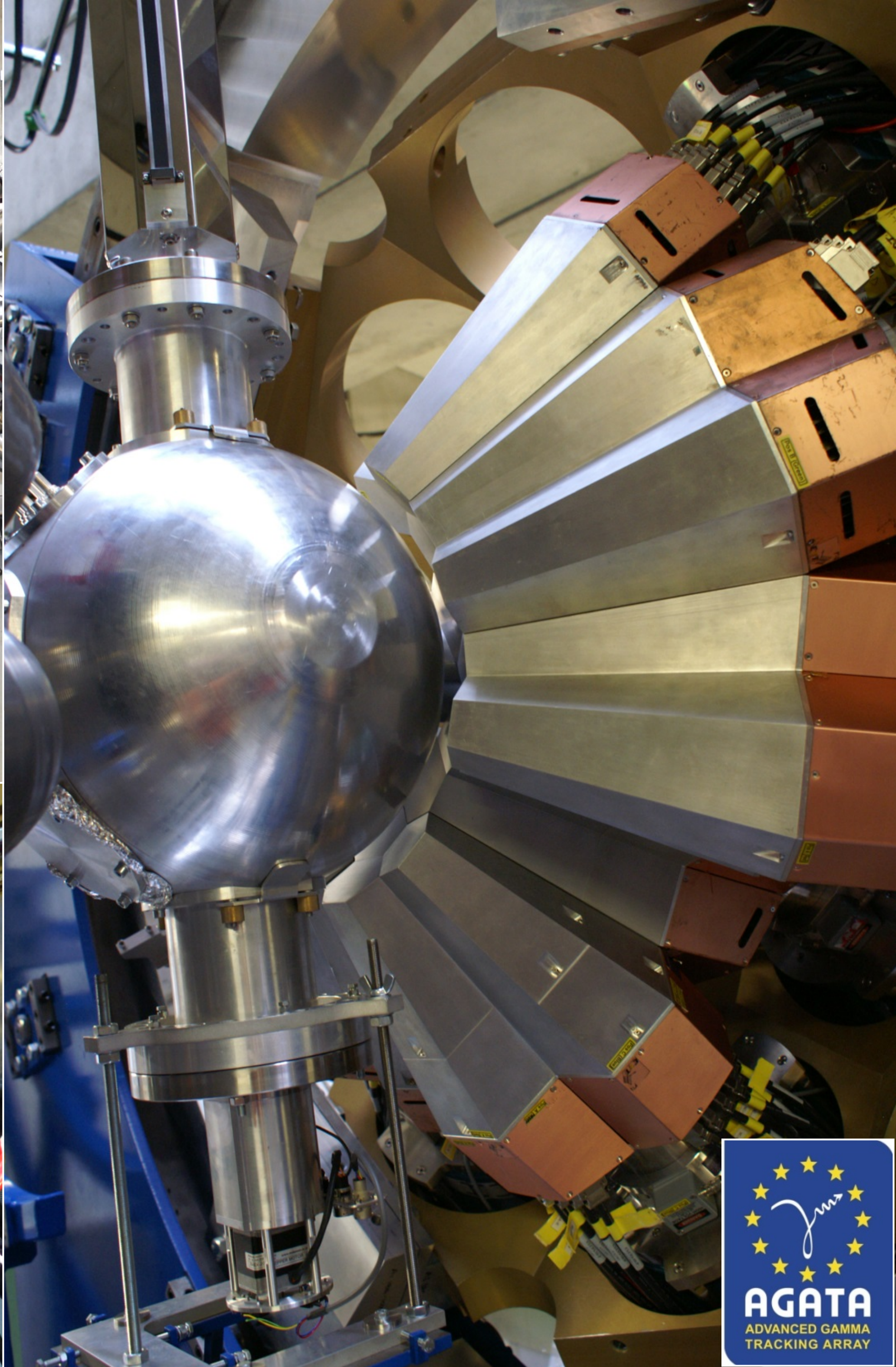
AGATA
ADVANCED GAMMA
TRACKING ARRAY

# AGATA at PreSPEC

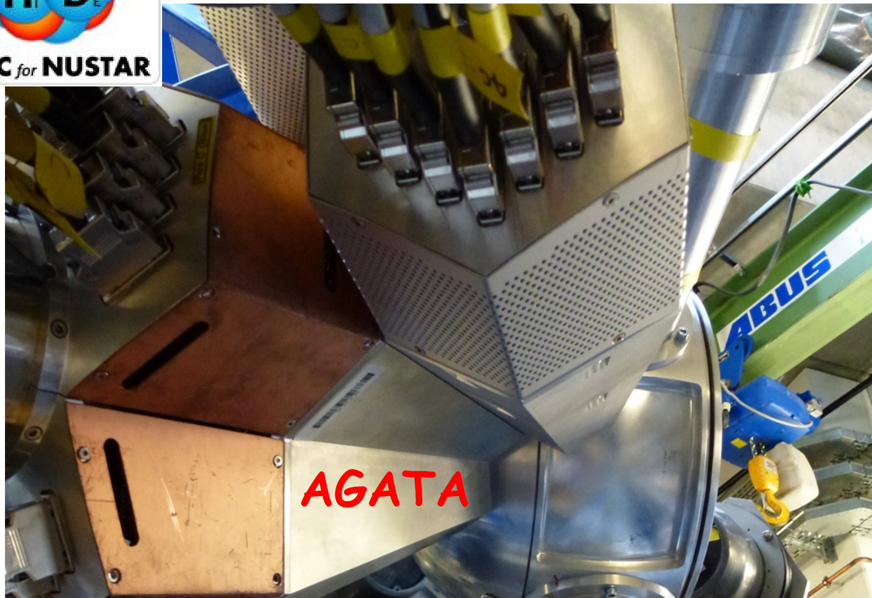


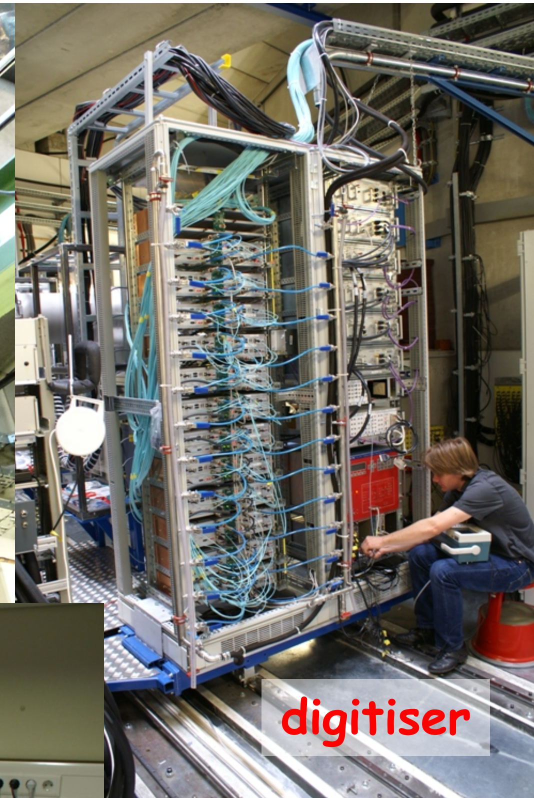



*Damian Ralet,*
*Stephane Pietri*

# Commissioning of $LH_2$ target

LH2 target used during the test in may 2011

- 2 cm thickness
- 7 cm diameter

Beam of $^{54}Cr$ at 150MeV/u

## Masse identification for Cr isotopes

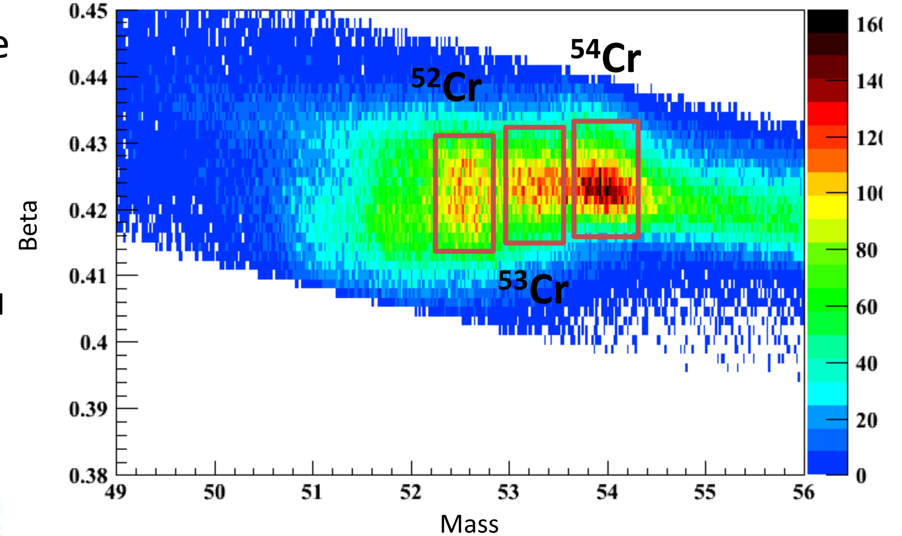


## Z identification

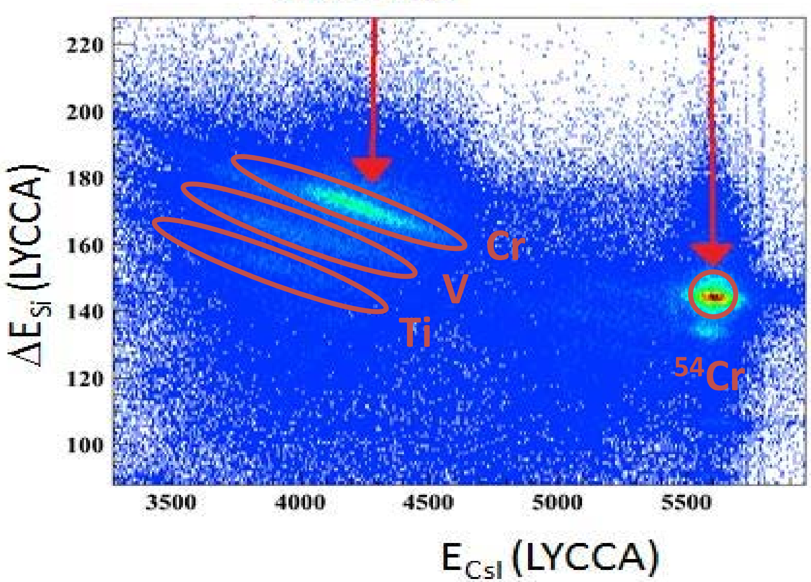


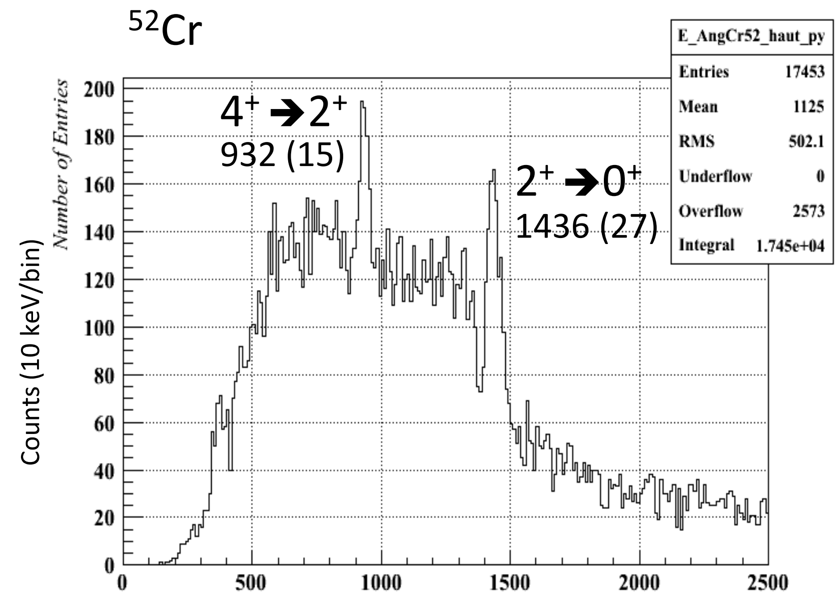

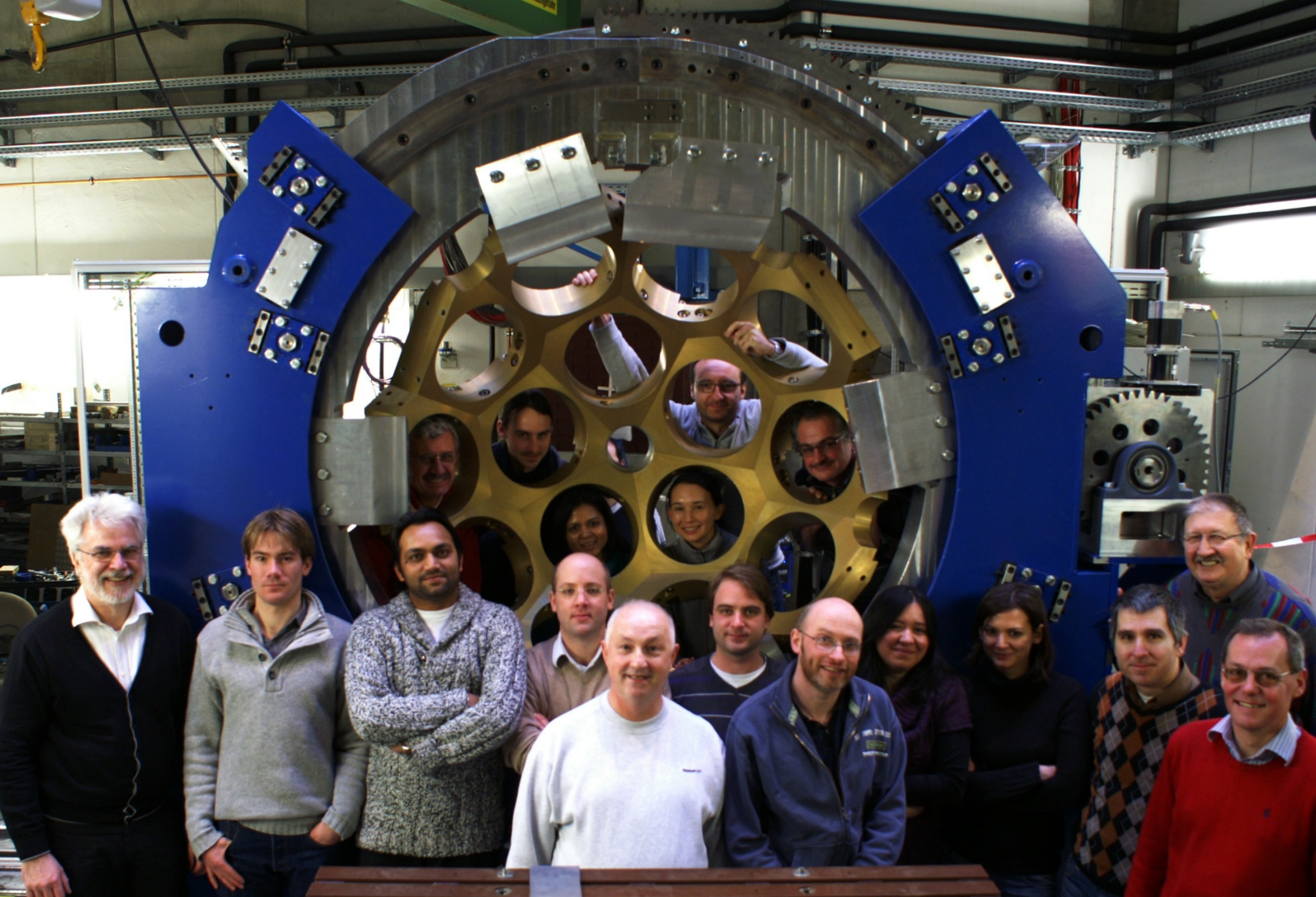

Ivan Kojouharov, Michael Reese, Namita Goel, Liliana Cortes, Frederic Ameil, Bogdan Szczepanczyk
H.-J. W., Damian Ralet, Pushpendra Singh, Stephane Pietri, Tobias Habermann, Edana Merchan, Giulia Guastalla, Plamen Boutachkov, Adolf Brünl
Ian Burrows, Jonathan Strachan, (Paul Morral), Jürgen Gerl, (Henning Schaffner, Magda Gorska)

# Reactions with relativistic radioactive beams – $R^3B$

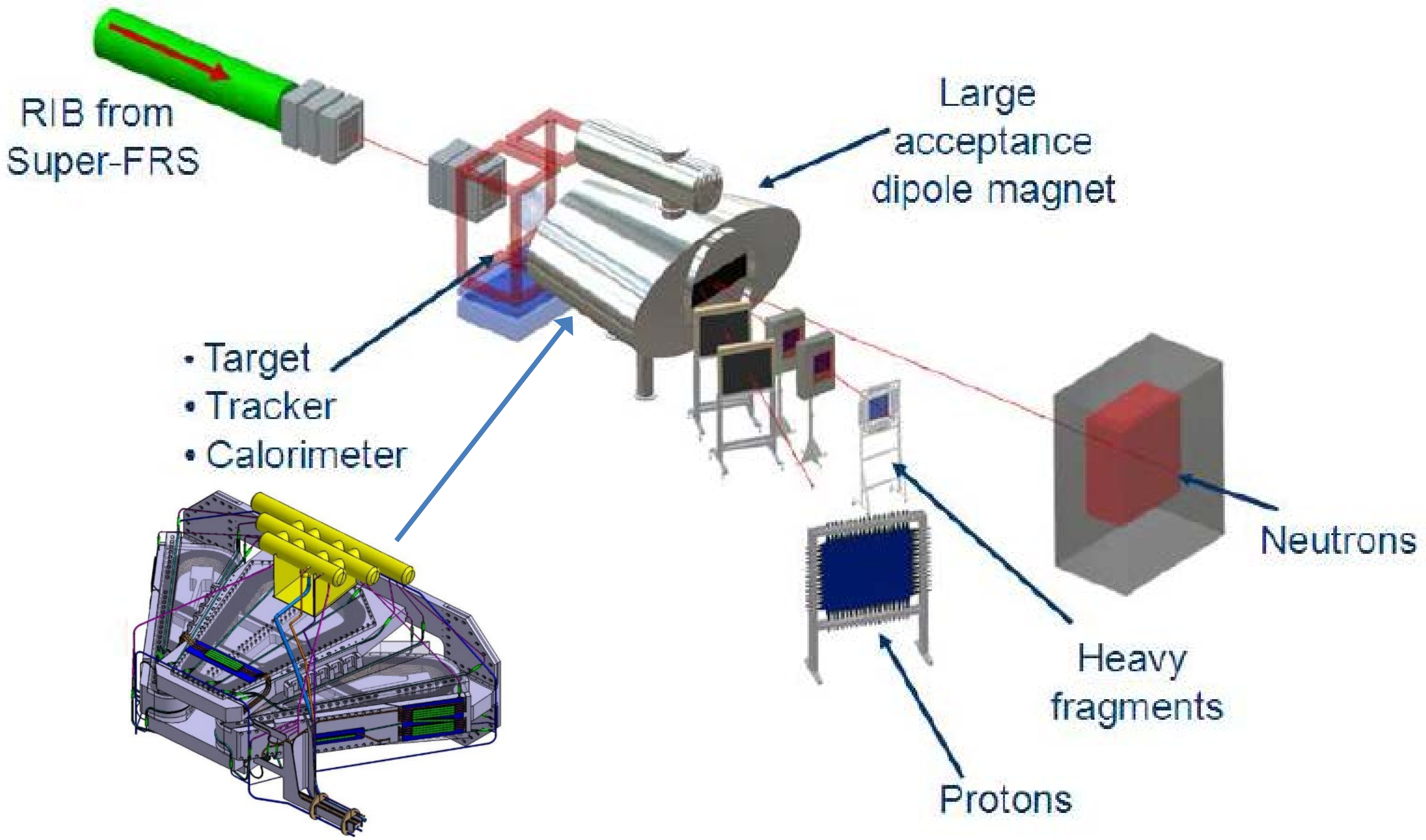


Excitation energy $E^*$ from kinematically complete measurement of all outgoing particles

$$E^* = \left( \sqrt{\sum_i m_i{}^2 + \sum_{i \neq j} m_i m_j \gamma_i \gamma_j \left(1 - \beta_i \beta_j cos\vartheta_{ij}\right)} - m_{proj} \right) c^2 + E_{\gamma,sum}$$

# Large Area Neutron Detector

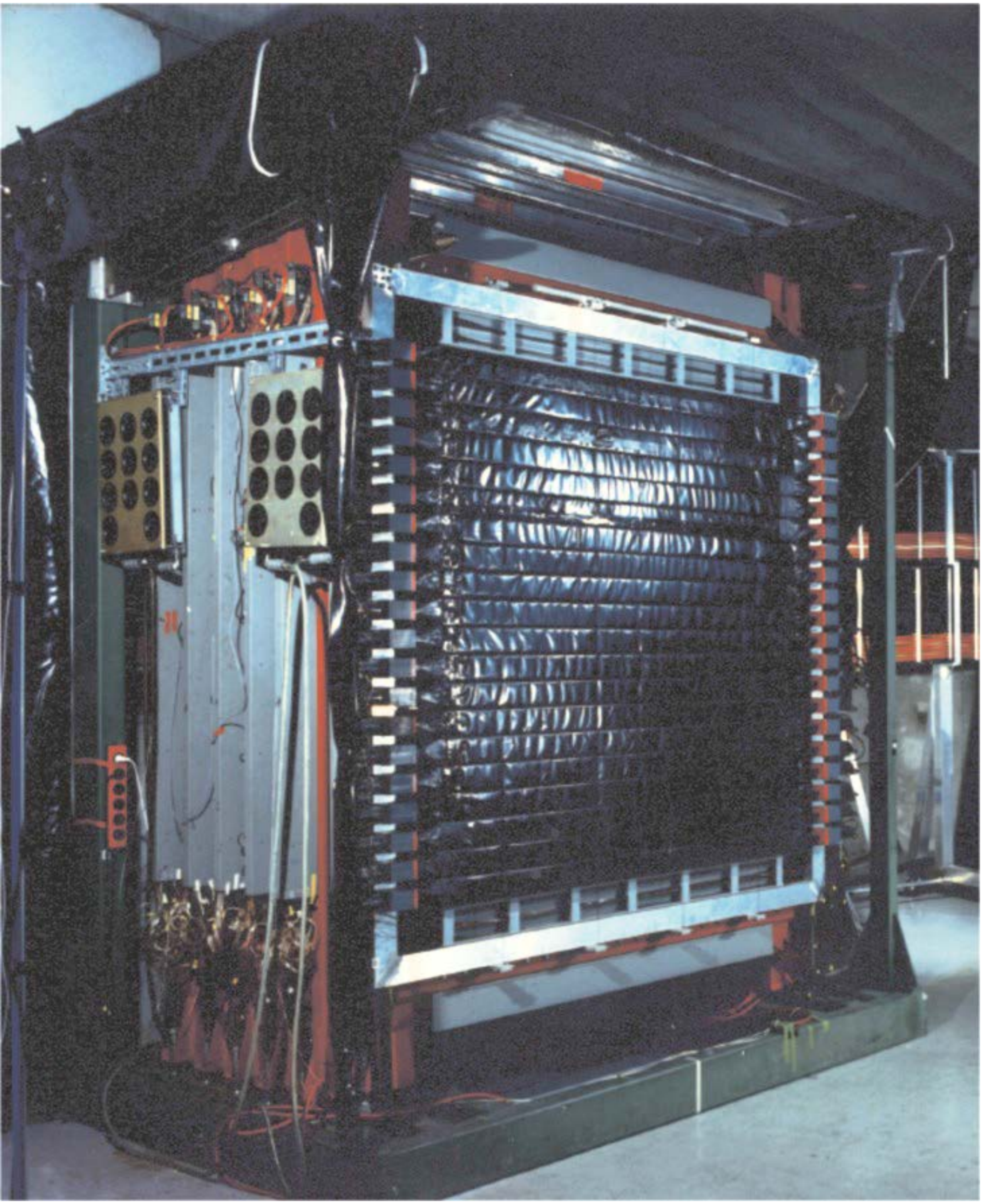

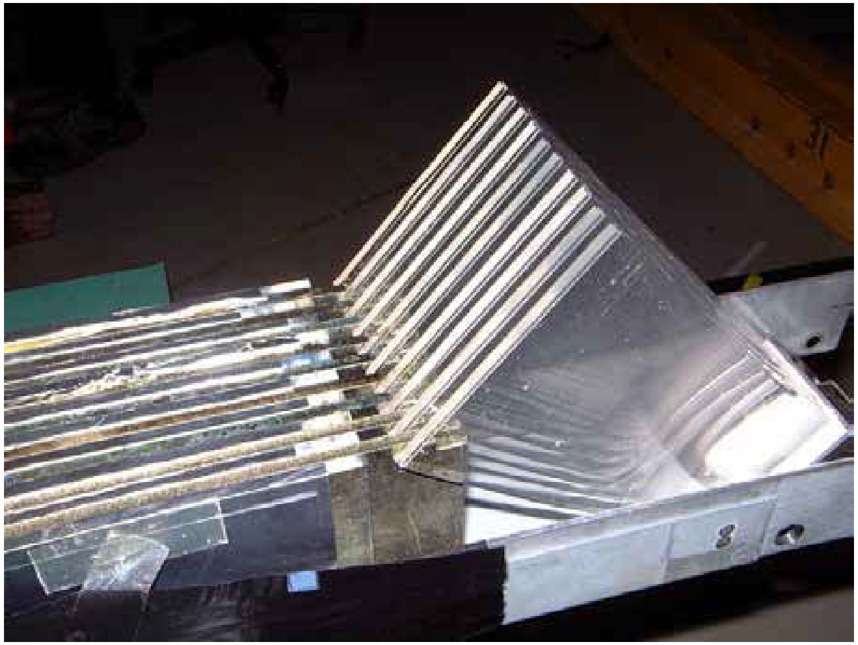

***L***arge ***A***rea ***N***eutron ***D***etector (2m x 2m x 1m)

- neutron energy $T_n \leq 1$ GeV
- $\Delta T_n/T_n = 5.3\%$
- efficiency ~1
- passive Fe-converter

# Invariant mass analysis

$$M_{proj}^{inv} = m_{proj} + E^*$$

$$M_{proj}^{inv} = \sqrt{\left\{ \begin{matrix} \left(\sum_i E_i\right) \\ \left(\sum_i \vec{p_i}\right) \end{matrix} \right\}^2}$$

$$\left(\sum_i E_i\right)^2 = \sum_i (\gamma_i m_i)^2 + \sum_{i \neq j} \gamma_i \gamma_j m_i m_j$$

$$\left(\sum_i \vec{p_i}\right)^2 = \sum_i (\gamma_i \beta_i m_i)^2 + \sum_{i \neq j} \gamma_i \gamma_j \beta_i \beta_j m_i m_j cos\theta_{ij}$$

$$M_{proj}^{inv} = \sqrt{\sum_i {m_i}^2 + \sum_{i \neq j} m_i m_j \gamma_i \gamma_j \left(1 - \beta_i \beta_j cos\theta_{ij}\right)} + E_\gamma$$

$$E^* = \sqrt{\sum_i {m_i}^2 + \sum_{i \neq j} m_i m_j \gamma_i \gamma_j \left(1 - \beta_i \beta_j cos\theta_{ij}\right)} - m_{proj} + E_\gamma$$

Momentum reconstruction: (ħ=c=1)

four-momenta: $\hat{P} = (E, \vec{p})$

$$\begin{Bmatrix} p_x = p_0 sin\theta cos\phi \\ p_y = p_0 sin\theta sin\phi \\ p_z = p_0 cos\theta \end{Bmatrix}$$

$$p_0 = m_0 \beta \gamma$$

$$\gamma^2(1 - \beta^2) = 1$$

# Dipole strength distribution of $^{68}$Ni

mean field calculation

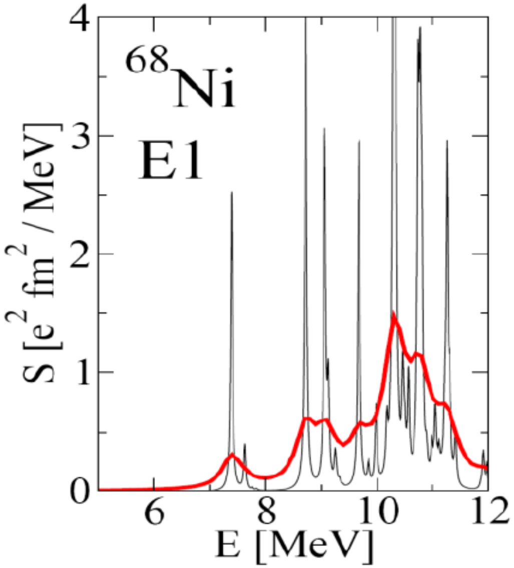


E.Litvinova et al.; PRC 79, (2009) 054312

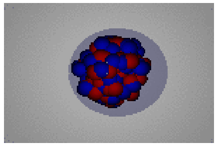

Pygmy resonance

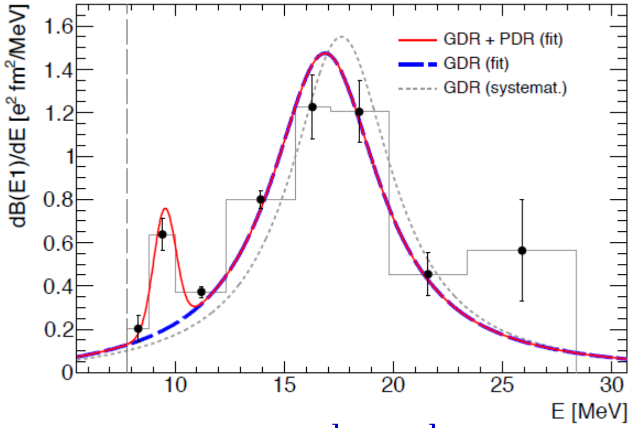


neutron decay data

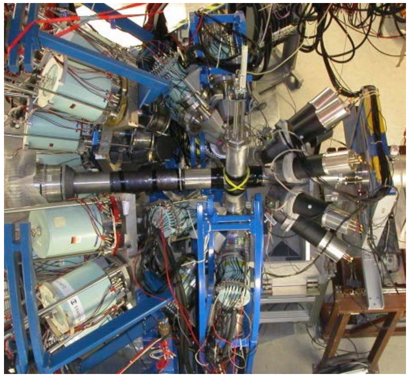

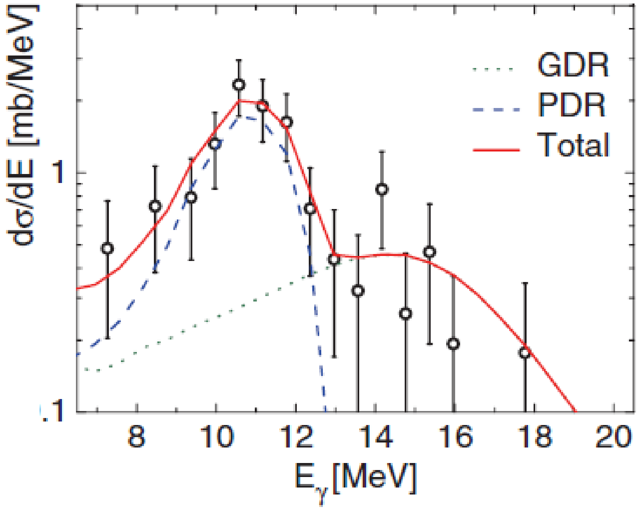


γ-ray decay data

direct γ-decay branching ratio:

$\Gamma_0/\Gamma = 7(2)\%$

O. Wieland et al.; Phys. Rev. Lett 102, 092502 (2009)

D. Rossi et al.; Phys. Rev. Lett 111, 242503 (2013)

# Slow down beams – new experimental perspectives

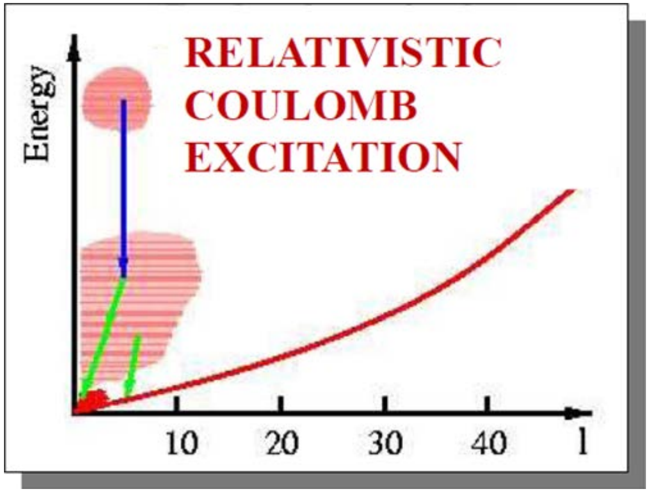


*collective strength*

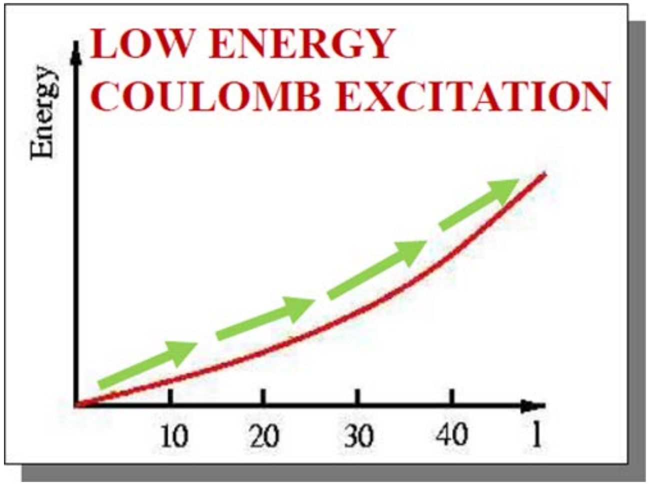


*nuclear shape*

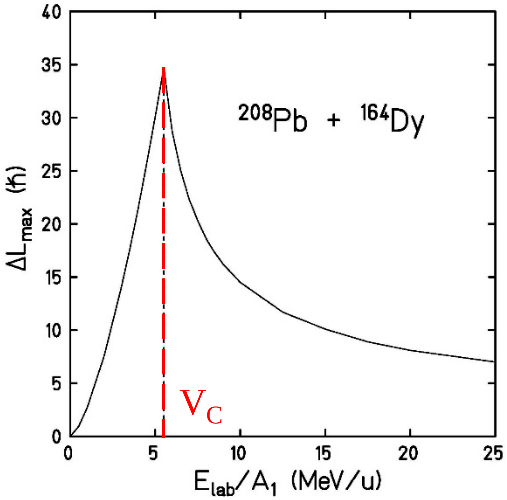


***angular momentum transfer:***

$$\Delta L_{max} \cong \frac{Z_P \cdot e^2 \cdot Q_0}{4 \cdot \hbar \cdot v \cdot a^2} \cdot (1 - cos\theta_{cm})$$

# Slowed down beams – beam characteristics

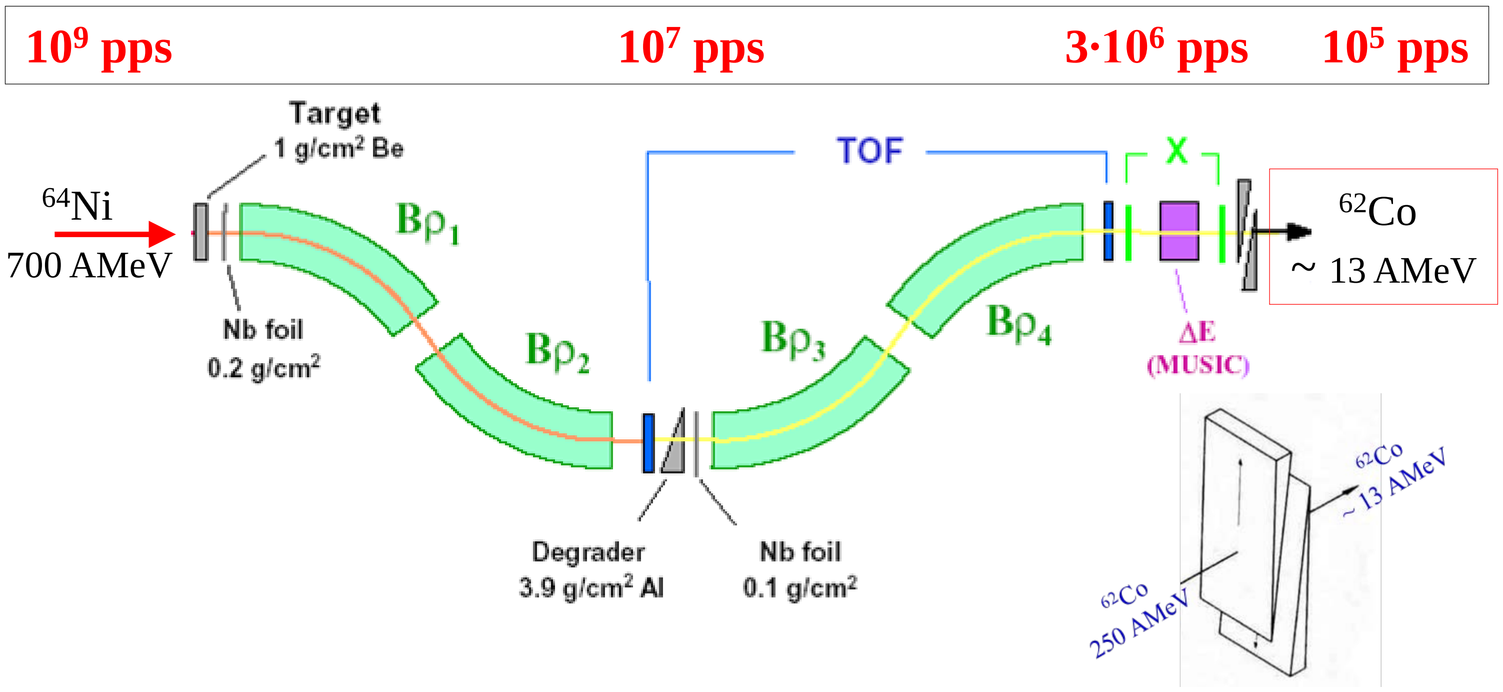


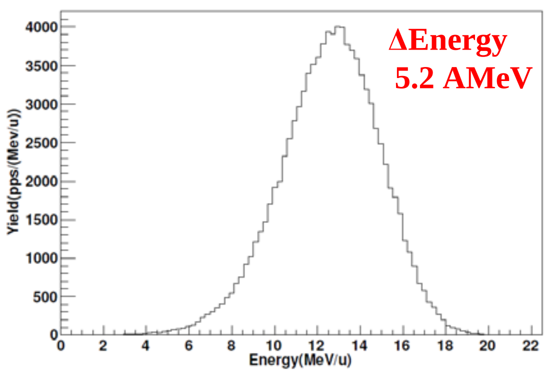


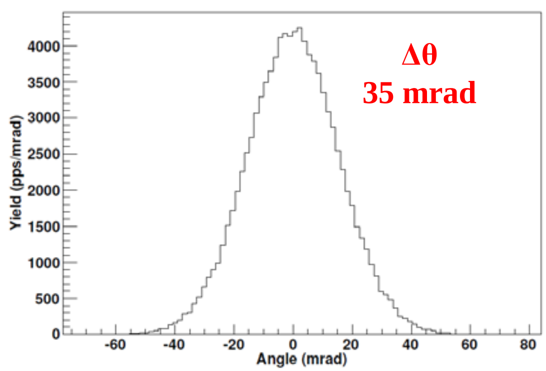


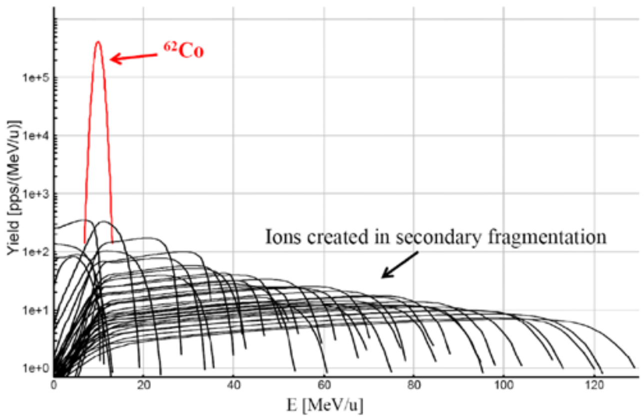

# Slowed down beams – experimental set-up

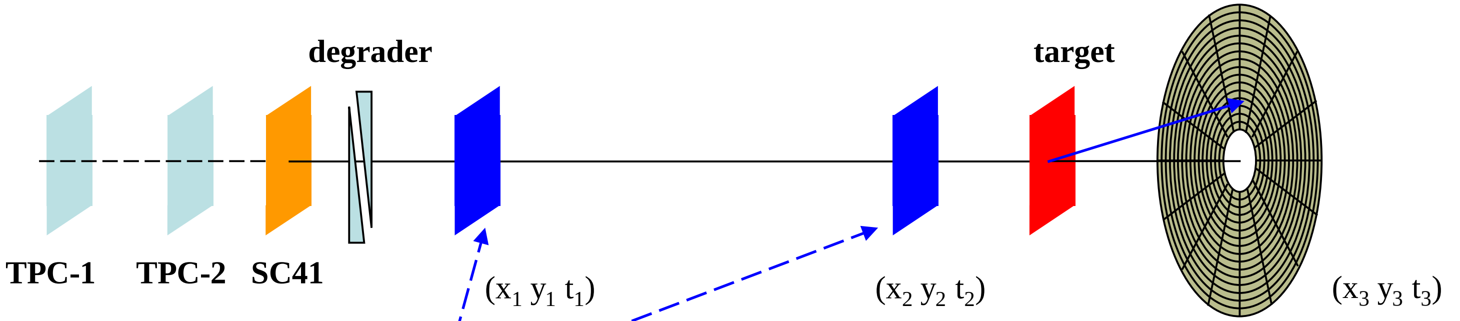


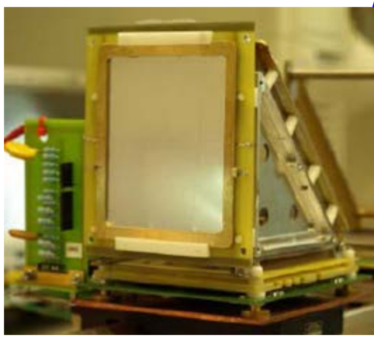

**electrostatic mirror + MCP detector**

position resolution ~ 1 mm
time resolution ~ 100 ps

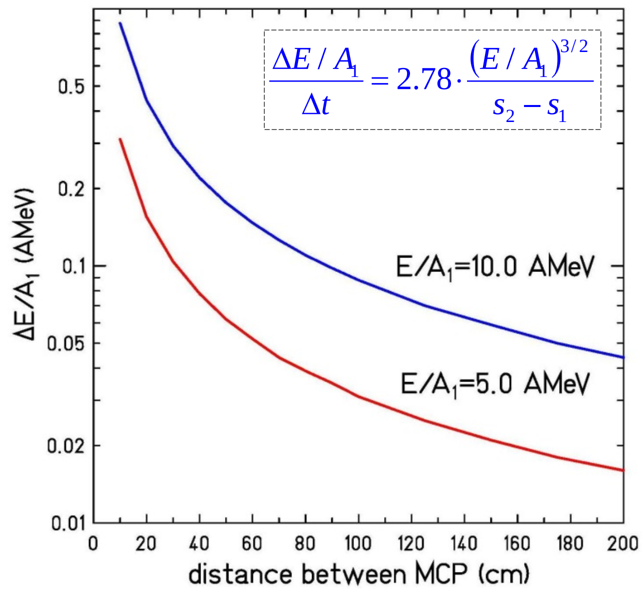


experimental results:

velocity β
beam energy $E/A_1$
scattering angle $\theta_{cm}$

MCP ≡ micro channel plate

# Slowed down beams – experimental set-up

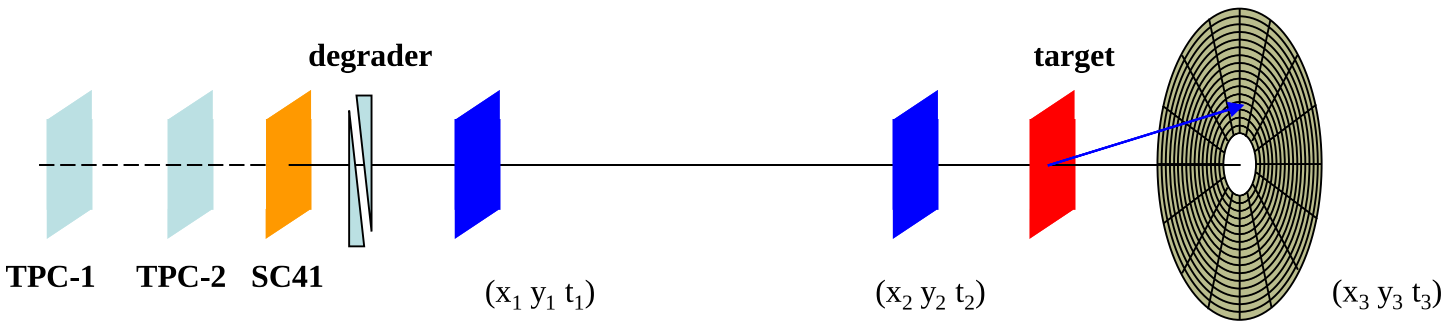


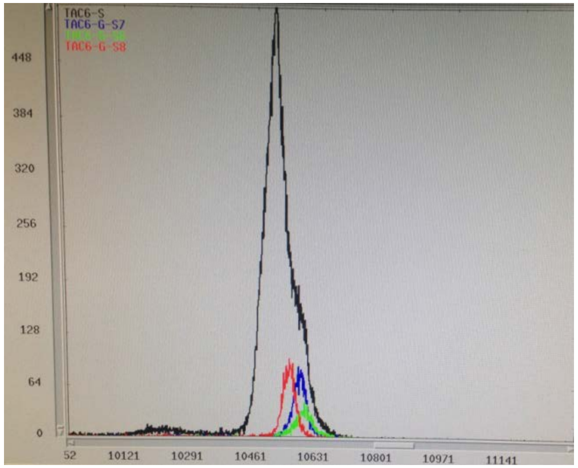


TOF between MCP and DSSSD

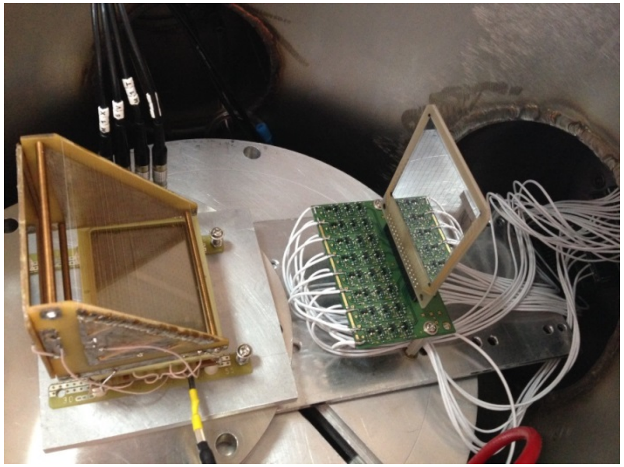

MCP DSSSD

**Time resolution 200 ps** for one of the 256 detector pixels

Akhil Jhingan (IUAC)

# FAIR accelerator facility